JOURNAL
OF THE AMERICAN CHEMICAL SOCIETY
Registered in U.S. Patent Office. © Copyright, 1975, by the American Chemical Society
VOLUME 97, NUMBER 24 NOVEMBER 26, 1975

A Simple Model of Hydrogen Bonding

Leland C. Allen

Contribution from the Department of Chemistry, Princeton University, Princeton, New Jersey 08540.
Received December 23, 1974

Abstract: A physical model of the hydrogen bond, A–H···B, has been deduced from ab initio molecular orbital wave functions of 36 dimers made from the monomers, NH_3, OH_2, FH, PH_3, SH_2, and ClH. Three monomer quantities are defined which characterize the model: μ_{A-H}, the A–H bond dipole; ΔI, the difference between first ionization potentials of the electron donor and the noble gas atom in its row; and l, the length of the hydrogen bonding lone pair. Dimerization energy, charge transfer, internuclear separation, directionality, stretching force constants (K_{AB} and K_{AH}), the dimer dipole moment, and ir intensity enhancement can be understood in terms of these quantities. The dimerization energy formula, $E_D = K\mu_{A-H}\Delta I/R$, where K is an energy scale factor and R, the internuclear separation between A and B, systematizes existing experimental and computational data. The tendency for strong bonding electron donors to be weak bonding proton donors and vice versa is the result of an intrinsic reciprocal relationship between μ_{A-H} and ΔI. Charge transfer is proportional to μ_{A-H} for specified B, and is ordered according to l for a given A. Internuclear separation is inversely proportional to μ_{A-H} for specified B, and has close to the same dependence on A–H for second- and third-row electron donors. The almost constant separation difference of 0.8 Å between second- and third-row electron donors results from the difference in average l between the rows. The rule of constant R for all B in a row (with given A) is found to arise from the constancy of l times I. Stretching force constants for the heavy atoms follow Badger's rule, $K_{AB}(R - d_{AB})^3 = 1.86$, with d_{AB} dependent only on the column of the periodic table. d_{AB} is 1.00, 0.80, and 0.55 Å for groups 5, 6, and 7, respectively. Lowering of the A–H stretching force constant, K_{AH}, relative to the monomer, is proportional to μ_{A-H} for fixed B, variable A, and proportional to ΔI (or l) for fixed A, variable B. The model also provides qualitative explanations and some quantitative results for the properties of other hydrogen bonds: the strong hydrogen bonds found in crystal ions, the weak hydrogen bonds to π electrons in organic molecules, the multiply bonded electron donors of proteins, a variety of substituents at A and B, and the cooperativity found in trimers and higher polymers. Quantitative predictions of E_D and R can be made for dimers formed with fourth-row hydride monomers.

Because of its well-established importance in chemistry and biology, a great deal is known about hydrogen bonding. A broad range of instrumental techniques has been applied and a moderately large number of ab initio quantum mechanical calculations have been carried out. There exist six books[1] and quite a few up-to-date review articles which treat both experimental and theoretical aspects.[2] Several significant insights have been gained from the quantum mechanical calculations, but three simple qualitative bonding descriptions have long dominated attempts to organize the experimental data. These are: (a) the two-term Mulliken charge transfer expression,[3] used by analogy with the more general class of donor-acceptor complexes,[4] (b) the set of four valence bond structures using hybridized atomic orbitals for the A–H bond and the B atom lone pair introduced by Coulson,[5] (c) the three-center, bonding, nonbonding, molecular orbital picture proposed in 1951 by Pimentel.[6] Each of these descriptions calls to mind a somewhat different view, but each has been successful in emphasizing important aspects of the hydrogen bond. Recent experimental and computational additions to the literature make it now possible to devise a more quantitative model and to bring together and extend the ideas inherent to the above three descriptions. Contemporary quantum mechanical results show that features from the whole of the A and B containing molecules are necessary to a complete understanding and the physical model proposed here is able to take these into account, thus going beyond the three-atom, three-center description generally associated with older viewpoints.

Physical models of structure and bonding have frequently proved useful in chemistry and physics, e.g., the crystal field theory model originally proposed by Bethe,[7] the Born model of ionic crystals,[8] the Lewis-Kossel octet model of chemical bonds,[9] London's simple formula for long-range dispersion forces,[10] the nuclear shell model,[11] and the spin wave-Heisenberg model of ferro- and antiferromagnetism.[12] Our approach has been to build a physical model expressed in terms of spectroscopically obtainable quantities for a set of

complete molecular systems. To treat the A and B atoms of greatest chemical interest, the molecular systems considered were the 36 neutral, linear dimers made from the NH_3, OH_2, FH, PH_3, SH_2, and ClH monomers. This set is taken to represent the normal hydrogen bond and the properties encompassed by the model are: dimerization energy, internuclear separation, directionality, stretching force constants, K_{AH} and K_{AB}, dimer dipole moment, charge transfer, charge redistribution, and the ir intensity enhancement. From this model of the normal hydrogen bond it is possible to make extensions to: the strong hydrogen bonds found in ions, the weak hydrogen bond formed with π electrons in organic molecules, multiply bonded electron donors, dimers of fourth-row hydrides, substitution of other groups for the hydrogens on A and B, and the nonadditivity found in trimers and higher polymers. The purpose of the model is to provide a conceptual framework for understanding trends and regularities in experimental data. Its intent follows a principal role suggested for theory in a recent essay by Hoffmann.[13]

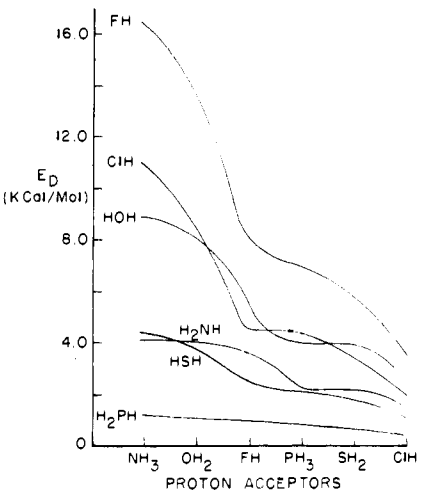

Figure 1. Dimerization energy vs. electron donors for 36 dimers calculated from molecular orbital wave functions with the 4-31G basis.

Quantum Mechanical Background

A. Data Available. Quantitative measurements have been made for a very large number of complex hydrogen-bonded systems, but in contrast to the well-developed literature of high-resolution spectroscopy for small covalently bound molecules which has been so important in the development of electronic structure theory for the covalent bond, a comparable body of experimental fact does not exist for gas phase dimers. There does exist, however, a moderate-sized literature of ab initio molecular orbital wave functions and these are taken as the numerical experiments from which our model is mainly constructed.

Almost all of the available ab initio wave functions employ the molecular orbital method. It is the consensus of the three articles which review theory[2] that the patterns and trends in hydrogen-bonding properties are adequately represented by this collection of results. The belief that the central features of the hydrogen bond are contained within the Hartree-Fock approximation has been further strengthened by recent calculations on $(H_2O)_2$ and $(HF)_2$ that give quantitative agreement with high-resolution spectroscopic measurements on internuclear separation, bond angles, and dipole moments and for the intermolecular and intramolecular normal mode frequencies of $(H_2O)_2$ and HCN···H-F.[14] This favorable situation was to be expected because instantaneous electron-electron correlation is a less severe problem in hydrogen bonds than in covalent bonds due to the fact that dimers separate into closed shell monomers and that use of fixed free monomer geometries has turned out to be a reasonable first approximation. A few direct estimates of correlation energies have been made and in no case have correlation effects modified conclusions about the direction of trends in the properties of normal hydrogen bonds. For $(OH_2)_2$, estimates range from 0.3 to 1.0 kcal/mol.[15] These considerations help assure us that use of available wave functions can lead to a realistic model. Further confidence comes from the fact that closely related values for the central parameters in our model can be derived from both calculated results and spectroscopic measurements.

The principal source of numerical results has been 36 dimer wave functions made from the monomers NH_3, OH_2, FH, PH_3, SH_2, and ClH. This set was constructed with 4-31G basis orbitals by two independent research groups and extensive checking and refining was carried out.[16,17] Two other data sets at higher accuracy, one using a Hartree-Fock AO basis,[18] the other a 6-31G* basis[19] which includes d polarization functions on A and B, are available for the nine dimers obtainable from NH_3, OH_2, and FH. Four dimers, $(H_2O)_2$, $(HF)_2$, H_3N···H-OH, and H_2O···H-NH_2, have been computed with quite extended bases (including d polarization functions on A and B and p polarization functions on hydrogens).[20] Each of these four different sets of numerical results as well as the five gas phase dimers which have been studied experimentally ($(FH)_2$, $(H_2O)_2$, $(NH_3)_2$, $(ClH)_2$, $(SH_2)_2$) display the same general trends in dissociation energy and geometry when the electron donor and the proton donor are varied. Dimerization energies, E_D, for the 36 systems computed at 4-31G are shown in Figure 1. E_D for a half-dozen of the 4-31G basis dimers have been determined also by the Boys-Bernardi counterpoise scheme as well as the standard, dimer total energy minus monomer total energies definition. E_D are lowered almost in proportion to their magnitude by this technique, and trends are completely preserved.

Two aspects of dimer geometry are of particular note. The first of these has to do with R, the heavy-atom internuclear separation. In general, ab initio molecular orbital calculations yield quite satisfactory results and computations using an extended basis predict R values to within 2%. 4-31G gives rise to an error twice this great, but it is one sided, always producing values slightly too short. In constructing our model, it is relative R values that are of interest and all data sets yield ratios in remarkable agreement with experiment. $R(H_2O)_2/R(HF)_2 = 1.07$ from measurement, 1.06 from 4-31G, 1.07 from 6-31G*, 1.04 from Hartree-Fock AO's, and 1.05 from the extended basis of Diercksen et al. A second aspect arises from the fact that most dimer calculations have assumed monomer geometries fixed at experimental values. Exploration of this approximation shows in situ proton movements of 0.01-0.02 Å (ΔE_D = 0.1-0.2 kcal/mol)[16] with the 4-31G basis set. These movements decrease smoothly as the basis quality is improved and become an order of magnitude less for the most elaborate bases. H_3N···H-Cl is the well-known exception, at 4-31G the proton movement is 0.1 Å (1.9 kcal/mol) and with a larger basis displacement to a midway position occurs. The H_3N···H-F proton displacement is a fourth as great (ΔE_D = 0.3 kcal/mol) and no others show anomalies. Thus for our purposes the use of monomer geometries frozen at experimental values is an entirely satisfactory approximation for E_D values but less satisfactory for force constant and intensity enhancement considerations.

First ionization potentials are an important property of electron donors and Table I gives experimental vertical ionization energies and values obtained by Koopmans' theorem with 4-31G wave functions. Relative to the other monomers, it is apparent that the calculated values for OH_2 and

Table I. Ionization Potentials (eV)

Monomer	Exptl[a]	ΔI[b]	Calcd[c]	ΔI[d]
NH_3	10.88	10.68	11.23	11.77
OH_2	12.62	8.94	13.59	9.41
FH	16.05	5.51	17.08	5.92
Neon	21.56		23.0[d]	
PH_3	10.60	5.16	10.38	5.42
SH_2	10.47	5.29	10.43	5.37
ClH	12.74	3.02	12.77	3.03
Argon	15.76		15.8[d]	

[a] H. J. Lempka, T. R. Passmore, and W. C. Price, *Proc. R. Soc. London, Ser. A*, **304**, 53. (1968). A. W. Potts and W. C. Price, *ibid.*, **326**, 181 (1972). [b] Difference between monomer and noble gas atom at end of a row. [c] Calculated with 4-31G basis. [d] Extrapolated values.

Table II. Monomer Dipole Moments (Debyes)

Monomer	Exptl[a]	Calcd[b]	Monomer	Exptl[a]	Calcd[b]
NH_3	1.47	2.28	PH_3	0.58	1.05
OH_2	1.85	2.61	SH_2	0.97	1.78
FH	1.82	2.28	ClH	1.08	1.86

[a] R. D. Nelson, D. R. Lide, and A. A. Maryott, *Natl. Stand. Ref. Data Ser., Natl. Bur. Stand.*, No. 10 (1967). [b] Calculated with 4-31G basis.

FH deviate from the observed ones by the largest amount. FH is most out of line (1.03 eV) and this yields calculated dimerization energies and ΔI that are too low relative to the other monomers.

The single most important issue in the available computed data is the relative accuracy of monomer properties between the second and third rows of the periodic table. A first concern is the lack of d functions in the 4-31G basis. This raises the question of a possible imbalance in representation between the two rows. Test of this hypothesis, however, has demonstrated that an imbalance does not occur for hydrides (but does for other ligands).[21] A second consideration is monomer dipole moments and the experimental moments along with 4-31G calculated values are given in Table II. It is apparent that the error for third-row monomers is twice that for the second row. This problem is particularly important for proton donors and in order to minimize the effect of the mismatch and to help bring out trends, an appropriate averaging method is indicated. Selection of the proper scheme is achieved by examining the plots of the raw computed data for E_D and r, Figures 1 and 2. A striking feature of both figures is the close similarity of values displayed by proton donors O and Cl and by N and S for all electron donors while values for proton donors F and P stand apart at opposite ends. In seeking an explanation for this observation, we first recall the long established relationship between hydrogen-bond strength and the proton-donor electronegativity.[1,2] In addition, it is well known that second- and third-row electronegativities show the diagonal relationship, a similarity in values along diagonal lines in the periodic table.[22] Ordering by the diagonal relationship is invariant among the numerous electronegativity scales that have been proposed.[23] These considerations thus suggest diagonal averaging of proton donor values, O with Cl and N with S, and this procedure considerably aids in analysis of the data and construction of the physical model. Figure 3, E_D vs. r(H···B), is an example. Smooth curves dependent only on the electron donor result from diagonal averaging and the relation between the several curves and the possibility of extrapolation becomes apparent.[24] It should be noted here that the validity and use of the model to be derived in this paper is not dependent on the diagonal relationship. However, this feature is inherent to the available data and helps in its chemical interpretation.

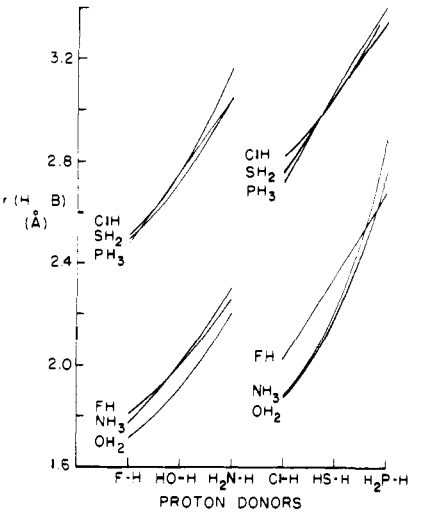

Figure 2. Internuclear separation, r(H···B), vs. proton donors for 36 dimers calculated from molecular orbital wave functions with the 4-31G basis.

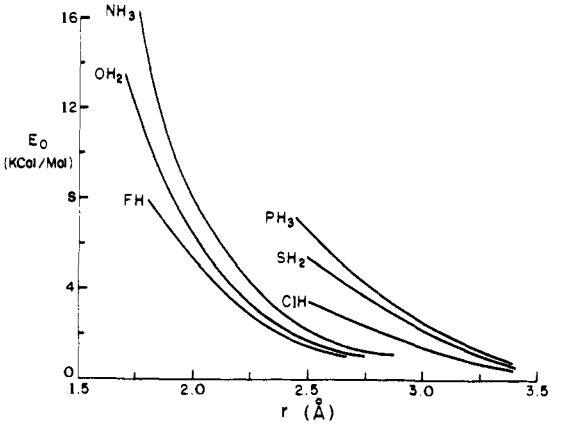

Figure 3. Dimerization energy vs. r(H···B) for the six electron donors calculated from molecular orbital wave functions with the 4-31G basis. Diagonal averaging employed for proton donor (HO-H values averaged with Cl-H and H_2N-H with HS-H).

It should also be stated that our data are for linear hydrogen bonds only. The fact that these are the usual form is supported both experimentally and computationally.[2] In some cases, e.g., $(HCl)_2$, both cyclic and linear configurations have been reported[25] with the linear form preferred. Recent calculations show the linear form approximately ½ kcal/mol more stable.[26]

B. Quantum Mechanical Aspects. Electron Donor Lone Pairs. The molecular orbital representation is taken for lone-pair orbitals. The electron donor lone pair important to hydrogen bonding is the highest occupied molecular orbital in each of the six monomers and its one-electron energy may be identified with the first ionization potential through Koopmans' theorem. For OH_2, SH_2, FH, and ClH these lone pairs are pure p_π, while in NH_3 and PH_3 they are an s,p mixture. However, the s orbitals in NH_3 and PH_3 have a greater radial fall-off rate than the p orbitals. Lone-pair angular dependence is shown by the polar plots in Figure 4. For OH_2, SH_2, FH, and ClH these are the familiar $2p\pi$ perpendicular to the molecular plane and for NH_3 and PH_3 the ordinary lone pair along the molecular symmetry axis projecting out from N and P. Lone-pair radial dependence

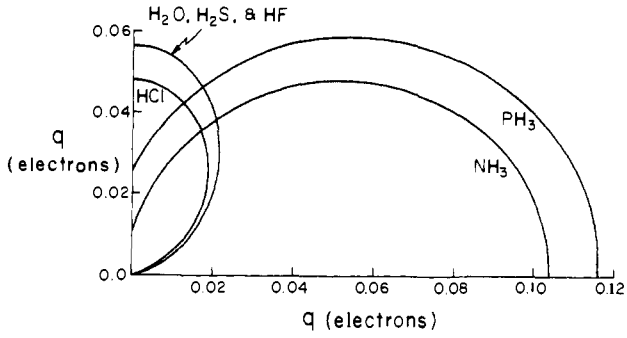

Figure 4. First quadrant polar plot of the angular charge distribution for the highest occupied molecular orbital in the six monomers calculated with the 4-31G basis. Angular variable is zero along horizontal axis and 90° along vertical axis. Contours shown are 90% enclosed charge.

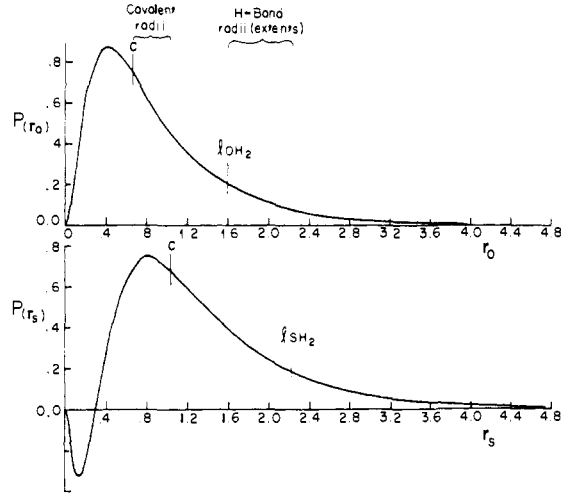

Figure 5. Radial amplitude function, $P(r)$, for oxygen in OH_2 and sulfur in SH_2 vs. r. Covalent radii from Pauling. Radial extent, l, from present work.

$rR(r) \equiv P(r)$ is displayed for OH_2 and SH_2 in Figure 5. As found with ordinary covalent bonds, the energy required to stretch a hydrogen bond by a given percent is much greater than that required for the same percent change in angle. For hydrogen bonds, radial changes are 10 to 15 times more energetic than corresponding angular variations and, in analogy to covalent radii, it proves useful to define a lone-pair radial extent. Any such definition is, of course, nonunique and we give data here for one that proves adequate to exemplify our model. The radial lengths or extent of the hydrogen-bonding electron-donor lone pairs tabulated in Table III represent that radial distance along the angular maximum which encloses 98% of the charge in the orbital.[27] These extents are independent of angle for OH_2, SH_2, FH, and ClH and vary only slightly with angle for NH_3 and PH_3. On the graphs of Figure 5, we have marked the extent positions (l) along with those for Pauling covalent (C) radii.[28] Hydrogen bonding is a phenomenon of the orbital tails, thus much less energetic than ordinary bonds. The characteristic exponential decrease in these orbital tails causes the difference between congener extents to be greater than those for covalent radii.

Further insight into the nature of these electron-donor lone pairs is obtained from potential energy graphs. A schematic of the effective potential around B is shown for FH, OH_2, and NH_3 in Figure 6 in order to point out the inverse relation between first ionization potential and radial extent.

Table III. Lone-Pair Extents, l (Å)

Monomer	l[a]	Monomer	l[a]
NH_3	1.77	PH_3	2.16
OH_2	1.58	SH_2	2.13
FH	1.35	ClH	1.95

[a] Calculated for 98% enclosed charge with 4-31G basis.

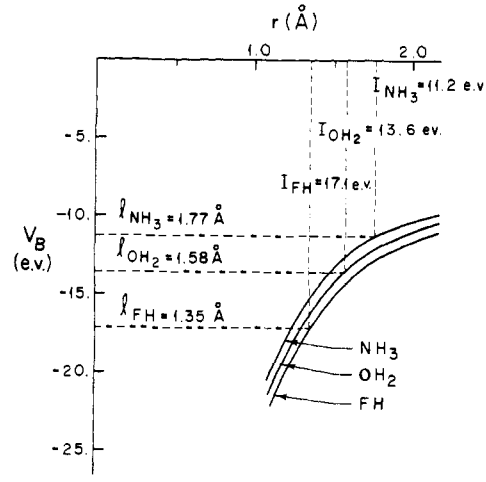

Figure 6. Schematic representation of the effective potential energy walls for 98% enclosed charge for electron donors NH_3, OH_2, and FH. Relationship between the radial extents, l, and the monomer ionization potentials for highest occupied molecular orbitals shown by dashed lines.

Proton Donor Bond Dipoles. When a monomer acts as a proton donor the bond dipole moment along the A–H bonds, μ_{A-H}, is a principal characterizing feature and we give here a prescription for relating it to the total monomer dipole moment. The sum of the projections of μ_{A-H} for each ligand along the molecular symmetry axis plus the effective dipole moment of the lone pairs along this line is equal to the observed monomer dipole moment. In the molecular orbital representation lone-pair contributions to the dipole moment come from those lone pairs with charge lobes lying along the symmetry axis and there is one of these in each of the six monomers. In FH, OH_2, ClH, and SH_2, the orbital energies of these lone pairs lie directly below the electron-donor hydrogen-bonding lone pair discussed in the previous paragraph while in NH_3 and PH_3, they are identical with the electron-donor hydrogen-bonding lone pair since these monomers have only one lone pair. The symmetry axis lone pairs show the same radial extent ordering as the highest occupied molecular orbital lone pairs and examination of the molecular orbital expansion coefficients suggests a relatively small contribution to the monomer dipole moment in HF, while in NH_3 the contribution is large and comparable to that from N–H bond dipoles. For simplicity and to minimize the number of assumptions, we take the contribution to the monomer dipole moment of the symmetry axis lone pairs to be zero for FH, 50% for NH_3, and half-way in between for OH_2. The same fractional contributions are employed for the third-row monomers. The reasonableness of this procedure for approximating μ_{A-H} can be inferred from the OH_2 charge density contours given as an example in Figure 7.[29] The $3a_1$ orbital is the symmetry axis lone pair and $1b_2$ is the main contribution to μ_{A-H} (the $p\pi$ electron-donor lone pair perpendicular to the molecular plane is omitted because it makes a negligible contribution to the bond dipole).

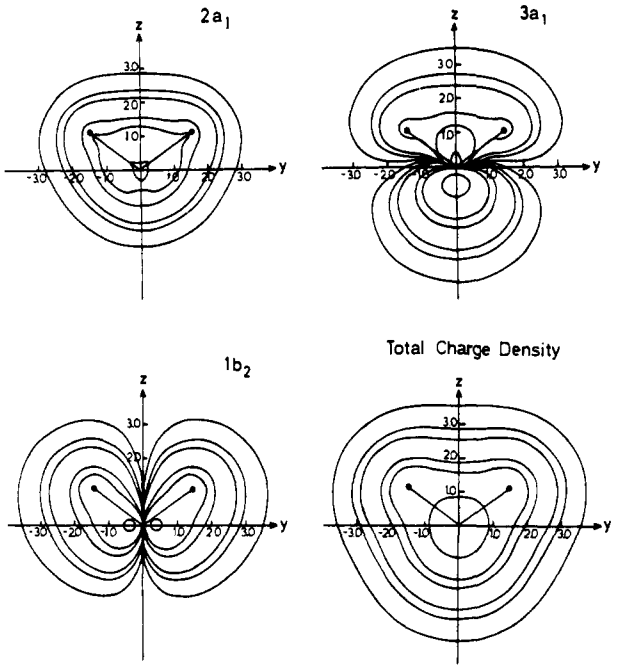

Figure 7. Orbital charge density contours in molecular plane for OH_2 (taken from ref 29). Distance in atomic units.

Model

A. Energy Formula. Because hydrogen-bond energies are small and the identity of the monomer in the dimers is largely retained, it is reasonable to expect that the dimerization energy can be expressed largely in terms of monomer parameters.[30] We show in this section how one can deduce a simple E_D formula depending on three spectroscopically accessible quantities.

There has been a long-standing belief that the chief characterizing feature of the electron donor is the ionization potential of its lone pair, but this has remained uncertain because of at least two difficulties. (a) The ionization potentials of some electron donors, such as OH_2 and ClH, are similar (12.62 and 12.74 eV, respectively) but their measured dimerization energies are quite different (5.2 and 2.1 kcal/mol, respectively), while the ionization potentials of OH_2 and FH are an order of magnitude further apart (12.62 vs. 16.05 eV) but the observed dimerization energies are closer together (5.2 vs. 7 kcal/mol). (b) The reciprocal of the ionization potential does not systematize E_D trends. These and related questions can be resolved by using the united atom ionization potential as a reference point. As an electron donor, the noble gas atom at the end of each row is assumed to form a hydrogen bond of zero energy and the ionization potentials of other electron donors are measured relative to this reference.[31] Lone pairs are created and B-H bonds are formed as the united atom is pulled apart. The corresponding lowering of the first ionization potential reflects the degree to which the lone pair is destabilized, i.e., made more available for hydrogen bonding.[32] Thus, ΔI, the difference between the first ionization potential of the monomer and that of the noble gas atom in its row (Table I) acts somewhat like the energy level splitting parameter in crystal field theory and it defines the lone-pair energetics. In addition to this role, ΔI measures lone-pair distortability, the extent to which the proton donor can induce a charge polarization of the electron donor. ΔI also provides a natural connection between electron donors in different rows of the periodic table. Third-row monomer ionization potentials are closer to argon than neon is to the second-row monomers, therefore third-row lone-pair orbitals interact less with A-H than their second-row congeners and lead to notably lower dimerization energies.[33]

Table IV. Bond Dipole Moments, μ_{A-H} (Debyes)

Bond	Exptl[a]	Calcd[b]	Diagonal av Bond	Diagonal av Exptl	Diagonal av Calcd
F-H	1.82	2.28	F-H	1.82	2.28
O-H	1.13	1.60	{O-H, Cl-H}	1.11	1.73
N-H	0.66	1.20			
Cl-H	1.08	1.86			
S-H	0.53	0.97	{N-H, S-H}	0.59	1.00
P-H	0.18	0.33	P-H	0.18	0.33

[a] Sum of μ_{A-H} projections along molecular symmetry axis equated to 1.0, 0.75, 0.50 of observed monomer dipole moment for FH, OH_2, NH_3, respectively, and for ClH, SH_2, PH_3, respectively. [b] Monomer dipole moments calculated with 4-31G basis at experimental geometry. μ_{A-H} determined as above.

The second quantity influencing dimerization energy is $1/R$ where R is the equilibrium separation between atoms A and B. Three lines of reasoning suggest this dependence. First, it is a gauge of the charge density since charge redistribution is occurring between A and H, in H···B, and between B and its ligands. Second, in a qualitative sense, one expects that bonding will be inversely proportional to the distance between the heavy atoms and this has been noted previously for some examples of ordinary covalent bonds.[34] The shorter equilibrium separations and larger dissociation energies of ionic hydrogen bonds likewise provide a limiting case outside the immediate domain of our model also pointing to a $1/R$ dependence. Third, the hydrogen bond is known to have an important electrostatic contribution[1,2] and the leading term in a classical multipole expansion is $1/R$ because charge distributions obtained from the available computed data show that the center of charge loss is between B and its ligands and the center of charge gain is near A.

To form a hydrogen bond, it is necessary that the proton donor have a bond dipole with the hydrogen slightly positive and the hydrogen orbital not entirely filled, and this is the third factor which comes into the E_D formula. The bond dipole may be taken as a measure of the electronegativity of A and a relation between these quantities and the bond strength has been long recognized.[1,2] A bond dipole definition was introduced in a previous section and Table IV lists the resulting bond dipoles obtained from both experimental measurements and 4-31G calculations of monomer dipole moments.[35] The diagonal relationship is at once apparent in these numbers and the diagonal averages are also tabulated.

The relationship between ΔI, $1/R$, and μ_{A-H} is brought out by plotting diagonal averaged E_D times R vs. ΔI using the 4-31G calculations (Figure 8). The four straight lines shown in this graph are close to a least-squares fit of the computed points. The slopes of all four lines are near to 1.64 times diagonal averaged μ_{A-H}. Thus the dimerization energy may be expressed as[36]

$$E_D = K\mu_{A-H}\Delta I/R \qquad (1)$$

where K is an energy scale factor that is 1.64 for the 36 dimers computed with the 4-31G basis.[37] The match to the 4-31G computed data achieved by eq 1 is best ascertained by plots of E_D vs. the proton acceptors and these are displayed in Figure 9. If the ΔI and μ_{A-H} obtained from experimental data are used in eq 1,[38] the match to computed E_D vs. BH_n is of equal quality to that shown in Figure 9. If diagonal averaging is not employed, the six curves generated by eq 1 show a vertical ordering: F-H, Cl-H, HO-H,

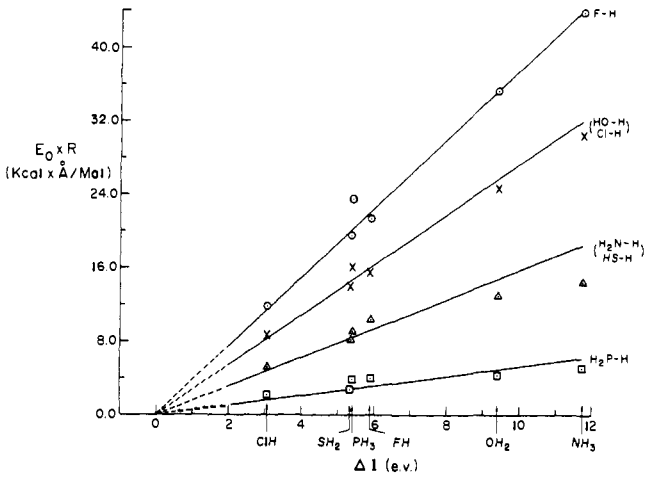

Figure 8. $(E_D)(R)$ vs. ΔI. Designated points are diagonal averaged values from 36 dimers calculated with 4-31G basis. Straight lines are approximate least-squares fit to computed values.

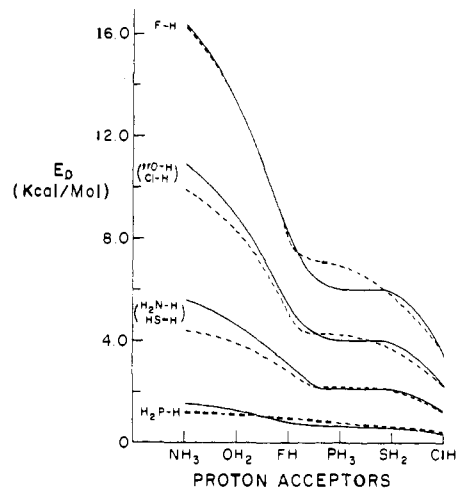

Figure 9. Diagonal average E_D vs. electron donors: (solid lines) E_D formula (eq 1); $K = 1.64$ (ΔI, μ_{A-H}, and R obtained from calculations using 4-31G basis); (dashed lines) results from 36 dimer molecular orbital wave functions using 4-31G basis.

H_2N-H, HS-H, H_2P-H for all B with Cl-H close to HO-H and H_2N-H close to HS-H. Overall, the match is quite comparable to Figure 9. Using ΔI and μ_{A-H} derived from experimental monomer dipole moments and R from the dimer wave functions, eq 1 is matched against computed E_D for the 6-31G* and Hartree-Fock AO data sets in Figure 10. The set of four high-accuracy E_D values obtained by Diercksen and collaborators[20] (H_3NHOH, 6.28 kcal/mol; $(H_2O)_2$, 4.84; $(HF)_2$, 4.5; H_2OHNH_2, 2.33) are close to those found with the Hartree-Fock AO basis and a comparable match can be obtained.[39]

Experimental E_D for the five gas phase dimers that have been studied are tabulated in Table V along with values determined from eq 1 using experimentally derived μ_{A-H} and ΔI.[40]

Kollman et al., in an important recent paper,[17] have predicted dimerization energies from monomer electrostatic potentials[41] with the 4-31G basis. Their results go a long way in providing an independent validation of eq 1. For a specified electron donor (NH_3) they computed electrostatic potential values produced by the six proton donors at a distance from the proton near to that of the hydrogen bond internuclear separation (2Å) and found them proportional to E_D. The electrostatic potential of the proton donor evaluated at the electron donor position should give a reasonable representation of the bond dipole and calculated μ_{A-H}, scaled to the electrostatic potentials of Kollman et al., are shown in Figure 11 (right). Electrostatic potentials arising from the six electron donors, with F-H as proton donor, were computed at 2.12 Å for the second-row electron do-

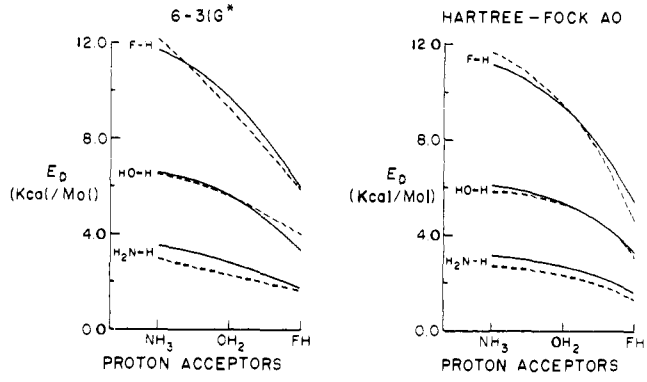

Figure 10. E_D vs. electron donors. Left side: (solid lines) E_D formula fit to $(H_2O)_2$; (dashed lines) nine dimers calculated with 6-31G* basis that includes d polarization functions on the heavy atoms (ref 19). Right side: (solid lines) E_D formula fit to $(H_2O)_2$; (dashed lines) nine dimers calculated with Hartree-Fock AO basis (ref 18). ΔI and μ_{A-H} derived from experimental ionization potentials and dipole moments employed in E_D formula for both right and left sections of figure.

Table V. Dimerization Energies (kcal/mol)

Dimer	Exptl	Eq 1[f]
$(FH)_2$	7.0 ± 1[a]	
$(OH_2)_2$	5.2 ± 1.5[b]	6.7
$(NH_3)_2$	4.5 ± 0.4[c]	4.0
$(ClH)_2$	2.14 ± 0.2[d]	1.5
$(SH_2)_2$	1.7 ± 0.3[e]	1.2

[a] E. U. Frank and F. Meyer, *Z. Elektrochem.*, **63**, 577 (1959). [b] H. A. Gebbie, W. J. Burroughs, J. Chamberlain, J. E. Harries, and R. G. Jones, *Nature (London)*, **221**, 143 (1969). [c] J. E. Lowder, *J. Quant. Spectrosc. Radiat. Transfer*, **10**, 1085 (1970). [d] D. H. Rank, R. Sitaram, W. A. Glickman, and T. A. Wiggins, *J. Chem. Phys.*, **39**, 2673 (1963). [e] J. E. Lowder, L. A. Kennedy, K. G. P. Sulzman, and S. S. Penner, *J. Quant. Spectrosc. Radiat. Transfer*, **10**, 17 (1970). [f] Equation 1 matched to $(FH)_2$. ΔI, μ_{A-H} derived from spectroscopic measurements, R from 4-31G calculations.

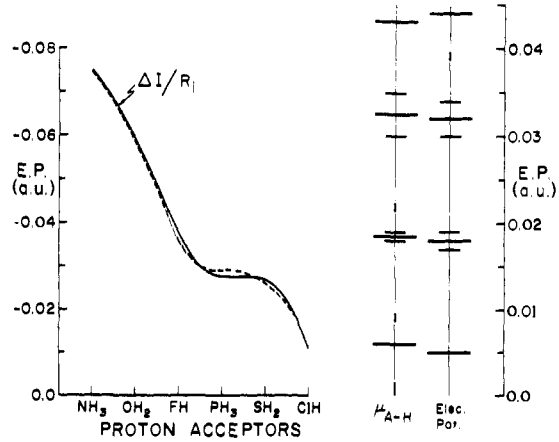

Figure 11. Electrostatic potentials computed from monomer wave functions using the 4-31G basis compared to model quantities also determined from monomer wave functions using the 4-31G basis. Left side: (solid line) $\Delta I/R_i$ referenced to F-H···NH_3. (Second-row average internuclear separation, $R_2 = 2.68$ Å, third row, $R_3 = 3.41$ Å); (dashed line) electrostatic potential computed at 2.12 Å from second-row electron donors and 2.65 Å from third-row electron donors (ref 17). Right side: μ_{A-H} referenced to HO-H···NH_3. Electrostatic potential for the six proton donors computed at 2 Å from H (ref 17).

nors and 2.65 Å for the third row and also found proportional to E_D. It is to be expected that the electrostatic potentials will give a good account of the calculated energy density, $\Delta I/R$. and a comparison is shown on the left side of Figure 11. The fact that the electrostatic potentials of Kollman et al. are able to successfully connect second- and third-row E_D values follows from a choice of positions for the potential energy evaluation which corresponds to the same percent of the total bond length for both rows. For proton donor F-H, the average R at 4-31G for the second row is 2.68 Å, the third row 3.41 Å, and this leads to the same fraction, 2.12/2.68 = 0.79 and 2.65/3.41 = 0.78, for both rows with the Kollman et al. position selections. Electrostatic potentials clearly afford a meaningful and inexpensive method for exploring extensions to eq 1 for cases such as electronegative substituents on A or B and aromatic π-electron donors.

There is another way of representing the electron donor in the dimerization energy formula. From Figure 6, as well as the data in Tables I and III, it is apparent that for each row there is a nearly linear relationship between l and ΔI. Thus a dimerization energy formula can be written in terms of $l - l_0$ instead of ΔI. l_0 = 0.91 and 1.44 Å for the second and third row, respectively, using the 4-31G basis with the 98% enclosed charge definition of l. For many electron donors more complicated than the hydrides, ΔI loses its identification with the charge lobe creating the hydrogen bond and a dimerization energy formula based on $l - l_0$ can often be used to extend the model to these cases.

There are several additional pieces of information that bear on eq 1 and lead to a further understanding of its nature. Kollman et al.,[17] in another part of their recent paper, have assumed an E_D relation of the form:

$$E_D = f(\text{A-H})g(\text{B}) \qquad (2)$$

determined f relative to NH_3 (and PH_3) as a standard electron donor for the six proton donors and g relative to F-H (and Cl-H) as a standard proton donor for the six electron donors. Using these standard electron donor-proton donor pairs as calibration, 25 of the 36 dimers may be predicted, and they found that comparison with 4-31G E_D values gave an average deviation of 0.6 kcal/mol. Equation 1 may be converted into the separable form of eq 2 by the approximation of replacing $1/R$ by $1/\langle l \rangle$, where $\langle l \rangle$ is the average lone-pair radial extent for a given row. Using the data from Table III, $\langle l \rangle$ is 2.33 Å for the second row and 3.11 Å for the third, and their ratio is 0.72. The corresponding $\langle R \rangle$ are 3.03 and 4.07 Å with ratio 0.81. This replacement leads to E_D vs. BH_n curves of the same shape and average deviation as the extrapolation procedures of Kollman et al. A separable equation of reasonable accuracy is possible because the principal numerical requirement on R is that it adequately represent the R discontinuity between second- and third-row electron donors and this, in turn, arises from the difference in lone-pair radial extents between rows. Equation 2 is also an adequate approximation when R only changes by a small percent.

The form of eq 2 immediately suggests comparison with the well-known relationship from classical electrostatics giving the interaction energy between proton donor and a proton acceptor proportional to the product of the monomer dipole moments weighted by the appropriate cosines and sines and inversely proportional to the cube of the separation between their centers of charge. Using experimental monomer dipole moments (Table II), the most reliable angles available from the quantum mechanical calculations, and a multiplicative energy scale factor constant, we obtain the E_D shown by the solid lines of Figure 12.[42] It is immediately apparent that a dipole-dipole electrostatic model is an inadequate representation of the hydrogen bond. This does not mean that dipole-dipole interactions play no part in hydrogen bonding (we discuss in a later section their major role in determining directionality) but rather that the pure electrostatic interaction between the two unperturbed monomer dipoles cannot explain binding energy trends nor other important features of the hydrogen bond. One may also inquire whether the proton donor function might better be represented by the full classical bond dipole expression thereby making E_D proportional to $(\mu_{A\text{-}H} \cos \alpha/R^2)(\Delta I)$ or $(\mu_{A\text{-}H} \cos \alpha/r^2)(\Delta I)$ rather than eq 1.[43] Both turn out to be notably inferior, overestimating the spread of E_D values for second-row electron donors and underestimating them for the third row.

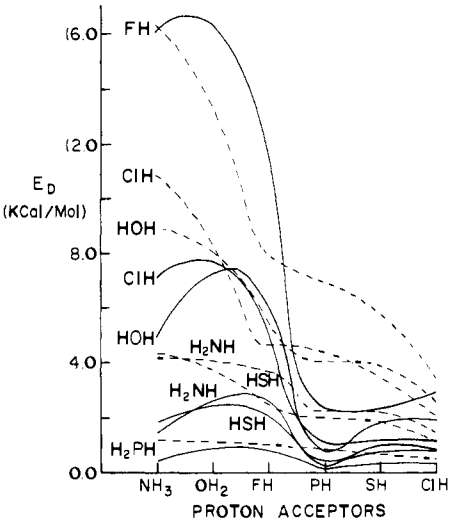

Figure 12. Solid lines: classical electrostatic energy between monomer dipole moments, referenced to E_D(HF···H-Cl) = 5.0 kcal/mol. Dashed lines: 36 dimers calculated with the 4-31G basis.

B. Charge Transfer and Lone Pairs. Charge transfer from the proton acceptor to the proton donor is a central feature of the charge rearrangement that occurs upon formation of a hydrogen bond. It helps determined directionality, dimer dipole moments, and ir intensity enhancement. In this section, we focus our attention on the electron donor half of the dimer and show that the transferred charge is controlled by l and the number of electron donor hydrogens.

Charge transfer is defined as the sum of the difference in Mulliken atomic populations between the dimer and proton acceptor monomer and, of course, is equal in magnitude but opposite in sign to the sum for the proton donor.[44] Values for the 36 dimers at equilibrium separation are displayed in Table VI. For each A-H, charge transfer decreases as electron donors are changed in the order NH_3, OH_2, FH for the second row, PH_3, SH_2, ClH for the third. On the average, charge transfer for second row electron donors is only 16% greater than for the third row and this is at first surprising since the ratio of second- to third-row average E_D is 2.25. The model quantity which organizes these patterns in charge-transfer magnitudes is the lone-pair radial extent, l.[45] Variation in lone-pair extent is shown vertically for two second-row proton donors in the schematic diagrams of Figure 13. These diagrams give r(H···B), R(A···B), and l to scale with l enclosed in ellipses to pictorially suggest a lone pair.[46] For fixed A-H variable B, internuclear separation is nearly constant within a row, thus producing a greater overlap of A-H and consequent greater charge transfer for NH_3 (PH_3) than FH (ClH). The effectiveness of charge transmission as ordered by l is complemented by the supply

Table VI. Charge Transfer (electrons)

A–H	BH_n	CT	BH_n	CT	BH_n	CT
F–H	NH_3	0.0425	OH_2	0.0310	FH	0.0301
O–H		0.0296		0.0266		0.0274
N–H		0.0216		0.0227		0.0219
Cl–H		0.0539		0.0368		0.0257
S–H		0.0322		0.0223		0.0154
P–H		0.0115		0.0096		0.0080
F–H	PH_3	0.0513	SH_2	0.0387	ClH	0.0249
O–H		0.0358		0.0263		0.0166
N–H		0.0231		0.0158		0.0071
Cl–H		0.0466		0.0307		0.0169
S–H		0.0229		0.0163		0.0101
P–H		0.0107		0.0076		0.0038

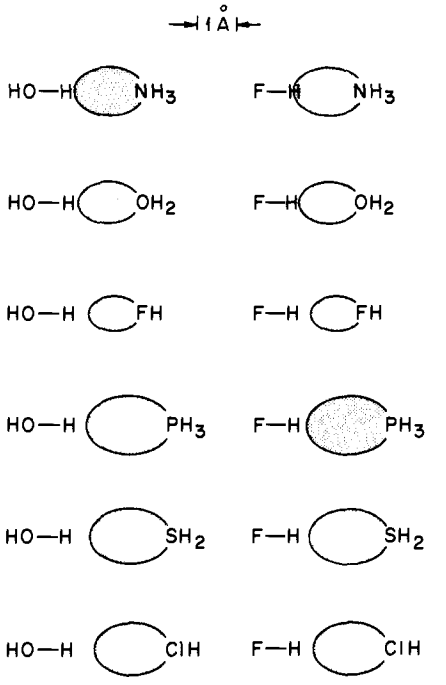

Figure 13. Scaled schematic showing relationship between R(A···B), r(H···B), and l for representative second-row proton donors. l equals length of shaded ellipse along horizontal axis.

of charge as ordered by the number of electron donor hydrogens. Charge-transfer differences within the third row are especially influenced by the number of hydrogens. Because both of these effects come into play, charge transfer is not linear in l and this brings out the fact that dimerization energy is not directly proportional to charge transfer. The similarity in charge-transfer magnitude between the second- and third-row electron donors is explained by the fact that the ratio of the l value average to the r(H···B) average is only 4% greater for the second than for the third row. Ultimately, this similarity in charge transfer arises because the difference in r(H···B) between rows is also set by the difference in l values.

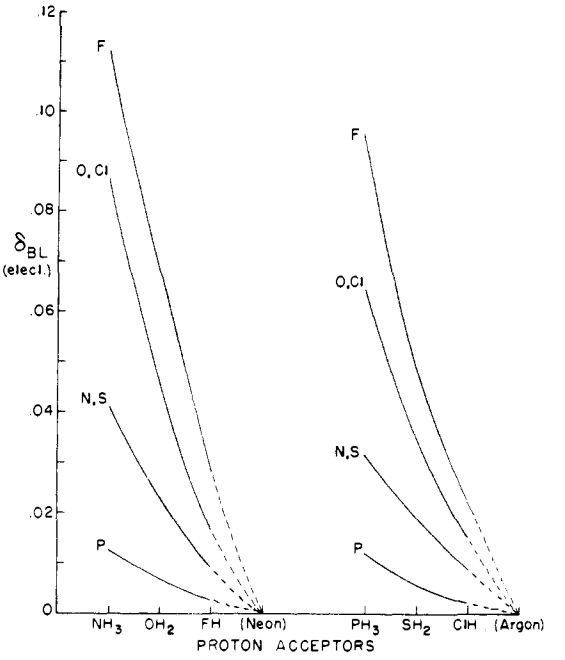

Figure 14. Charge change of electron-donor hydrogens for diagonal averaged proton donors vs. the six electron donors.

The effect of the lone pair is further revealed by calculations at nonequilibrium geometries. If a fixed R(A···B) is imposed on a set of dimers, then the lone-pair determines both charge transfer and the charge change on A, δ_A.[47] Representative results for three electron donors are listed in Table VII. For NH_3 $\theta = 0°$ and for OH_2 and SH_2 $\theta = 90°$, so that a fixed reference relative to the lone-pair orbital is maintained for these nonequilibrium geometry calculations.[48] The distance from A to the end of the lone pair, $R - l$, is constant in each of the three sets and CT and δ_A show approximate constancy for varying A–H. The approximate constant for the third row is greater than for the second because r(A–H) for the third row is uniformly larger than for the second, thus the lone pair is penetrating through a larger fraction of the A–H bond.

Even though the lone pair orders the pattern of charge transfer, the charge is principally provided by the hydrogen ligands of B.[44] The change in charge on the B ligands, δ_{BL}, is plotted for diagonally averaged A–H in Figure 14. δ_{BL} supplies the charge on B as well as the charge transfer[44] and the smooth extrapolation to zero charge change for the united atoms shown by the dashed lines is strong support for the choice of this ΔI reference in our model. Because charge density difference contours show both increases and decreases close to each other near B, δ_B sometimes misrepresents charge rearrangement effects,[44] but it does show the expected smaller buildup of negative charge for third-row compared to second-row B and this is reflected in δ_{BL}.[49]

C. Charge Redistribution and μ_{A-H}. In this section, we show how the proton donor influences dimer charge rear-

Table VII. Charge Transfer and Charge Change on A for Fixed R(A···B) (electrons)

A–H	BH_n	CT	δ_A	BH_n	CT	δ_A	BH_n	CT	δ_A
F–H	NH_3	0.037	−0.075	OH_2	0.040	−0.050	SH_2	0.028	−0.021
O–H		0.030	−0.074		0.041	−0.062		0.028	−0.025
N–H		0.021	−0.069		0.041	−0.066		0.026	−0.025
Cl–H		0.076	−0.168		0.086	−0.114		0.055	−0.056
S–H		0.072	−0.132		0.088	−0.113		0.047	−0.055
P–H		0.085	−0.138		0.099	−0.145		0.044	−0.055
		R(A···N) = 2.95 Å			R(A···O) = 2.87 Å			R(A···S) = 3.69 Å	

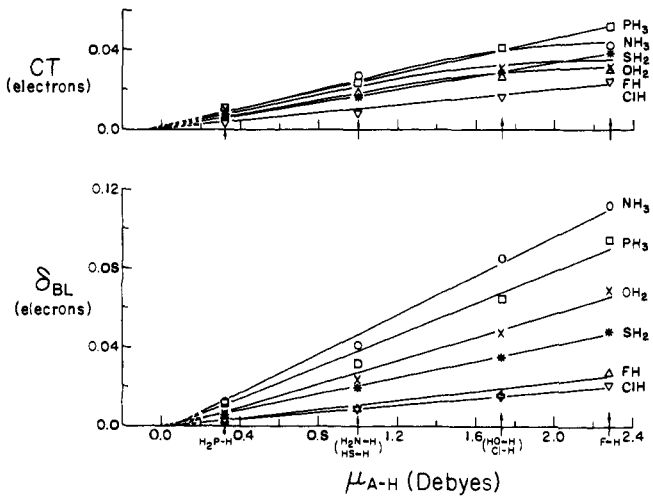

Figure 15. Diagonal averaged charge transfer and diagonal averaged charge change on electron-donor hydrogens vs. diagonal average μ_{A-H}. Points are computed values for 36 dimers employing the 4-31G basis.

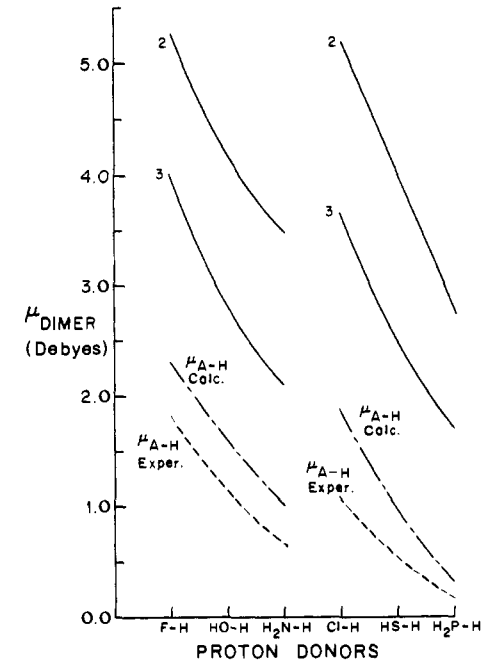

Figure 16. Dimer dipole moments for average electron donor of second row, 2, and third row, 3, vs. proton donor for 36 dimers computed with the 4-31G basis.

rangement and that μ_{A-H} is its driving force. There is a large buildup of negative charge on A due to charge transfer and to the loss of charge on H. Practically all of the charge flow occurs along A-H, the ligands of A participating in a secondary way.[50]

Returning to Table VI, we now consider trends within the columns (fixed B, variable A-H) and it is apparent that charge transfer follows μ_{A-H}. The origin of this pattern is shown by the scaled schematic diagram of Figure 13 through left-to-right comparison. Large μ_{A-H} means that the H orbital is less occupied and the lone pair can penetrate further.[51] Comparison between rows within the columns of Table VI displays the diagonal relationship and suggests plots of diagonal averaged CT and δ_{BL} versus diagonal averaged μ_{A-H} for the 36 dimers at equilibrium separation (Figure 15). Even though CT and δ_{BL} both come from the electron donors, it is apparent that they are almost directly proportional to μ_{A-H} and extrapolate (dashed lines) to zero values for zero μ_{A-H}. The reason for this is that μ_{A-H} controls equilibrium internuclear separation as well as A-H penetration. (Figure 15 is not in conflict with the ability of the lone pair to govern CT and δ_A at nonequilibrium fixed R(A···B) or fixed A-H.) δ_A is also proportional to μ_{A-H}, but only within a row, and it does not extrapolate to zero μ_{A-H}. Two factors are making δ_A slightly more complicated than CT and δ_{BL}: (a) the lone pair is present even if μ_{A-H} is very small and it pushes charge off H onto A; (b) the electronegativity of third-row elements is closer to H than the second row, resulting in small monomer charges on H, and during hydrogen-bond formation there is a greater charge shift from H to A for the third row.

Dimer Dipole Moment. Because of the exaggerated magnitudes and somewhat erratic behavior of calculated dimer dipole moments, the dipole moment curves shown as Figure 16[52] were averaged over the electron donors for each row to bring out the relation between the second and third rows.[53] The abscissa is laid out as an equally spaced array for the six proton donors to display the parallelism between the experimentally based and computationally based μ_{A-H} as well as the parallelism between μ_{A-H} and μ_{dimer}. If the same data are plotted as diagonal average μ_{dimer} vs. diagonal average μ_{A-H}, two nearly parallel straight lines result. The nearly linear relation between μ_{A-H} and dimer dipole moments comes about because δ_{BL}, CT, and δ_A are nearly linear in μ_{A-H}. Second-row dimer dipole moments are larger than those for the third row because third-row angles are uniformly larger than second-row values and the dipole moment of the proton donor is adding less or subtracting more from the electron donor dipole moment.

Summary of the Dimer Charge Redistribution and Energetics. The information from previous sections can be combined to give an overall picture of the charge redistribution produced by hydrogen bonding. The energy level of the electron donor lone pair is higher than the electron acceptor, charge transfer occurs, and the charge density in the H···B region is reduced because of the Pauli principle repulsions between the two closed shell monomers. Polarization of both the electron donor and proton donor occurs with considerable enhancement of μ_{A-H}. The resultant electrostatic interaction is a principal origin of the bonding. For a given electron donor at equilibrium separation, charge transfer and the charge distribution on both donor and acceptor is governed by μ_{A-H}. Because charge change on A-H and BH_n is a linear function of μ_{A-H}, the dimerization energy is a linear function of μ_{A-H}. For a given proton donor at equilibrium separation, charge transfer and δ_A is ordered by the lone-pair extents, l. The resultant charge redistribution on A-H varies with electron donors in the same manner as the dimerization energy.

The rule that a strong bonding electron donor will be a weak bonding proton donor and vice versa is manifest in the model; μ_{A-H} is proportional to χ_A and from the Mulliken definition of electronegativity,[54] χ_A is proportional to I. Large I means small ΔI and l, thus μ_{A-H} and ΔI or μ_{A-H} and l are reciprocally related. For two monomers in a given row, the question of which will be the electron donor and which the proton donor in the lowest energy dimer follows straightforwardly from relative acid and base strengths. However, intuitive predictions are more difficult for mixed dimers made from monomers of different rows. A determination is easily made from the E_D formula and the fact that E_D depends linearly on μ_{A-H}, ΔI, and l aids qualitative reasoning.

These patterns and trends generally fit with those found by other workers. Del Bene[55] has emphasized the major contribution made by the electrostatic effects, and Popkie,

Kistenmacher, and Clementi[14] have applied Clementi's bond energy analysis to their near Hartree-Fock water dimer wave function. At equilibrium separation, they find that the entire stabilization is obtained by the charge redistribution within BH_n and within the A-H containing monomer, that on HO-H being somewhat greater than on OH_2. Bowers and Pitzer[56] have made a bond orbital analysis of $(H_2O)_2$ which gives prominence to charge transfer and suggests that overlap repulsion may be of almost equal magnitude but opposite sign to the electrostatic energy. Duijneveldt and Murrell[57] have made calculations on the three-center fragment, A-H···B, using a perturbation theory for long-range intermolecular forces with nonnegligible orbital overlap. Four hybrid orbitals mounted on centers A and B are specified by their percent s character, χ_A and χ_B, respectively. Bonding and antibonding A-H orbitals mix a hydrogen 1s with the A hybrid via an ionicity parameter, k, and computations with A and B equal to N, O, and F were carried out to simulate the nine hydride dimers. Because of the several approximations introduced, these semiempirical wave functions are less accurate than the several sets of ab initio SCF results now available but they do yield dimerization energies ordered by the electron donor sequence $NH_3 > OH_2 > FH$, by the proton donor sequence $F-H > HO-H > H_2N-H$, and for a common electron donor, internuclear separation becomes shorter as the bond becomes stronger. These authors found that their results could be characterized by k and χ_B and these parameters bear a significant relationship to μ_{A-H} and l, respectively. Plots of both experimentally and computationally derived μ_{A-H} vs. k are linear with a negative slope. Consrtruction of an E_D times R vs. k graph from their data yields a fan-shaped set of curves arising from a common point that resembles the mirror image of our E_D times R vs. μ_{A-H} results. The proportionality between charge transfer and μ_{A-H} finds its correspondence in a greater charge transfer energy for smaller k. A smaller percent s character implies large radial extent, l, thus their finding that charge-transfer energy decreases with increasing χ_B parallels our Figure 13 and the approximate inverse proportionality between χ_B and E_D for second-row electron donors is in accord with the linearity we find between l and E_D. Dreyfus and Pullman,[58] Morokuma,[59] Duijneveldt and Murrell,[57] and Kollman and Allen[60] have decomposed the dimerization energy into various components, that of Morokuma and Duijneveldt and Murrell being the most complete. The detailed decomposition results of these research efforts differ considerably among each other and are subject to the well-known sensitivity to difference in basis sets. It is clear that detailed decomposition schemes will provide an increasingly important test of our model as more decompositions obtained from extended basis wave functions become available.

Hagler and Lifson[61] have derived a classical consistent-force-field potential for the amide hydrogen bond from heats of sublimation, dipole moments, and geometries of nine molecules and their crystals. They find that except for negligibly small nonbonded hydrogen parameters, ordinary nonbonded Lennard-Jones parameters along with free monomer Mulliken atomic charges fit the experimental data. The general conclusions from quantum mechanical calculations that to a first approximation monomers retain their electronic identity, that monomer geometries are unchanged, and that hydrogen loses charge all help validate the Hagler-Lifson potential function. The internuclear separation dependence assumed in our model, the use of electron donor and proton donor parameters derived from monomer quantities, and the possibility of characterizing charge transfer in terms of these parameters are likewise consistent with and supported by their results.

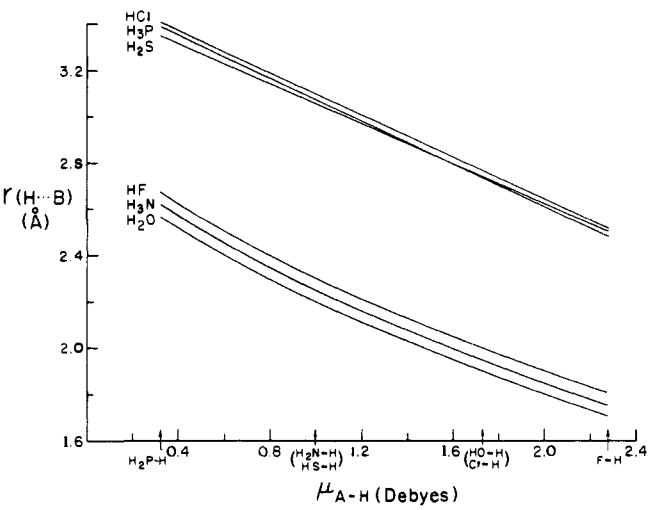

Figure 17. Diagonal averaged r(H···B) vs. diagonal averaged μ_{A-H} for 36 dimers computed with 4-31G basis. (Off-line points at r = 2.89 and 2.75 Å are $H_2P-H\cdots NH_3$ and $H_2P-H\cdots OH_2$, respectively.)

D. Internuclear Separation. Several striking patterns relating to internuclear separations are apparent in the computed data (e.g., Figure 2) and in this section we show how they can be explained with the proton-donor and electron-donor quantities already introduced.

For a given electron donor, the equilibrium internuclear separation is governed by μ_{A-H}. A large μ_{A-H} pulls the A–**H** bond charge strongly to A allowing the lone pair to penetrate further along A–H thereby resulting in a short r(H···B).[62] The scaled schematic diagrams in Figure 13 were used in the previous section to explain charge transfer, but they also display the pattern of internuclear separation and left-to-right comparison shows that larger μ_{A-H} leads to shorter r(H···B). A correlation for all 36 dimers is shown as diagonal average r(H···B) vs. diagonal average μ_{A-H} in Figure 17.[63] Manifestation of the diagonal relationship is complete and compelling in the connection between r(H···B) and μ_{A-H} because each quantity independently displays it clearly (Figure 2 and Table IV, respectively). Figure 17 brings out three important properties of r(H···B) that are taken up in turn: the almost common curve shape for second- and third-row electron donors, the vertical separation between rows, and the approximate constancy of r for all electron donors in a row. Since r is almost independent of B for a given row, the change in r as A varies over the six proton donors results almost entirely from the change in μ_{A-H}. Thus r changes by practically the same amount and has close to the same curve shape for electron donors of both rows, leading to an almost constant separation between rows. As can be seen in Figure 17 or in the original computed data, Figure 2, the magnitude of this separation is ≈0.8 Å and its origin is the difference in lone-pair radial extents between rows. Because the curves for different B are so close together, we take the difference between the l values averaged over a row and this value will be proportional to the average r separation between rows. It is less than 0.8 Å because the hydrogen of third-row proton donors is more fully occupied than in the second row making the difference in average l values approximately two-thirds the difference in average r values. Another measure which shows the relationship between the vertical displacement in r and l values is the ratio of r averaged over the 18 dimers with second-row B to the 18 dimers with third-row B compared to the ratio of averaged l for the second and third rows. This ratio is less dependent on the definition of l and these ratios are 0.73 and 0.75, respectively.

Table VIII. Internuclear Separation Measure[a]

BH_n	l	l^2l	BH_n	l	l^2l
NH_3	19.9	35.2	PH_3	22.4	48.4
OH_2	21.5	33.9	SH_2	22.2	47.3
FH	23.1	31.1	ClH	24.9	48.6

[a] Calculated values, using the 4-31G basis set, are used for all quantities in this table.

Constant *R*, Variable B. The approximate equality of r for all B in a row is apparent in the raw computed data of Figure 2 and the vertical columns of Figure 13 as well as Figure 17. This is a general property found in all available data sets[64] and is a sharp contrast to the large variation in r(H···B) when A is changed that was discussed in the paragraph above. The origin of this phenomenon lies in the similarity in form of the effective potential energy around B. A connection with model quantities can be obtained by assuming an analytic form for the potential. If it is taken as Coulombic:[65]

$$V_B = K_B/r$$

and since $V_B = I_B$ at $r = l_B$,

$$V_B = l_B I_B/r$$

From Table VIII it is apparent that $l_B I_B$ is approximately constant for a given row, thus making the effective potential seen by the proton donor almost independent of B. That equilibrium separation for a given A-H should be determined by the ll product is physically reasonable. The longer the length of the lone pair, l, the further away interaction will set in, but lone-pair length must be modulated by relative strength and a measure of this is ionization potential, I.

Another plausible analytic potential may be chosen from the form known for atoms at intermediate and larger distances:[66]

$$V_B = K_B'/r^2$$

and again $V_B = I_B$ at $r = l_B$, thus

$$V_B = l_B^2 I_B/r^2$$

Table VIII shows that $l_B^2 I_B$ is also approximately constant for a given row, again leading to a potential nearly independent of B for a specified row. It is likely that the actual potential around B is near to the analytical forms treated here and the variation in these two measures is the same as that shown by R from the computational results.[67]

E. Directionality. There are two important facts about the directionality of the hydrogen bond which set the focus of discussion. First, very small energies are involved, a large change in angle corresponds to a few tenths of a kilocalorie. These small magnitudes mean that the dimerization energy formula, eq 1, can contain no angle information. Second, currently available experimental and computational data do not support the hypothesis that the hydrogen bond lies along the maximum of the electron-donor lone pair for B equal to O, F, S, or Cl, either along the $p\pi$ orbital of Figure 4 or along valence bond sp^3 hybrids.[68] In this section, we again use the quantities previously introduced and show that directionality can be understood as a balance between the intrinsic stabilization along the lone-pair direction and interaction between the enhanced dipoles of the proton acceptor and proton donor.[69]

Variable A-H, Fixed BH_n. Figure 4 shows that NH_3 and PH_3 lone pairs have their maximum density along $\theta = 0°$, and those for OH_2, FH, SH_2, and ClH have their maximum density at 90°. If the orbital electron density alone were involved, maximum charge transfer and maximum stabilization energy would occur along $\theta = 0°$ for NH_3 and PH_3 and along 90° for OH_2, FH, SH_2, and ClH. The other factor that needs to be considered is the effective dipole-dipole interaction[70] between the electron donor and proton donor which tends to favor $\theta = 0°$. The resultant angle is a competition between these two effects (Table IX). For electron donors NH_3 and PH_3 orbital amplitude maximum and dipole moment direction coincide and $\theta = 0°$ for all proton donors. For electron donors OH_2, FH, SH_2, and ClH the orientation of the proton donor dipole moments is the largest contributing factor and similarity in congener angles is thus obtained. Because μ_{A-H} is determined by monomer dipole moment orientation and magnitude and because μ_{A-H} is the driving force for electron donor and proton donor dipole moment enhancement, the magnitude of μ_{A-H} simulates, for a given row, the effective proton donor dipole moment. Therefore, for a specified electron donor, the ordering of θ is inversely proportional to μ_{A-H} for A in a given row.

Table IX. Directionality (deg) (Variable A–H, Fixed BH_n)

A–H	BH_n	θ	BH_n	θ	BH_n	θ
F–H	NH_3	0	OH_2	0	FH	30
O–H		0		36		60
N–H		0		55		70
Cl–H		0		0		45
S–H		0		20		50
P–H		0		60		75
F–H	PH_3	0	SH_2	70	ClH	70
O–H		0		70		80
N–H		0		80		80
Cl–H		0		65		70
S–H		0		70		75
P–H		0		85		80

Table X. Directionality (deg) (Variable H_nB, Fixed H–A)

H_nB	H–A	θ	H–A	θ	H–A	θ
H_3N	H–F	0	H–O	0	H–N	0
H_2O		0		36		55
HF		30		60		70
H_3P		0		0		0
H_2S		70		70		80
HCl		70		80		80
H_3N	H–Cl	0	H–S	0	H–P	0
H_2O		0		20		60
HF		45		50		75
H_3P		0		0		0
H_2S		65		70		85
HCl		70		75		80

Variable H_nB, Fixed H–A (Table X). As before, the common direction of dipole moment and lone pair always produces $\theta = 0°$ for H_3N and H_3P. For H_2O compared to HF, the larger monomer dipole moment of H_2O (calcd 2.61 D vs. 2.28 D) means that dipole–dipole interaction is more heavily weighted thus leading to lower angles. For H_2S and HCl the monomer dipoles are close together (calcd 1.78 D and 1.86 D) and angles are correspondingly close. For both rows, the charge redistribution changes leading to H_nB dipole enhancement are greater than charge-transfer differences, thereby preserving the order according to monomer dipole moment. Equilibrium angles for third-row H_nB are higher than for the second row because monomer dipoles are smaller for third-row H_nB.[71]

F. Stretching Force Constants, K_{AB}. It is instructive to compare the force constants of ordinary covalent bonds and hydrogen bonds by use of Badger's rule:[72]

$$K_{AB}(R - d_{AB})^3 = 1.86 \qquad (3)$$

K_{AB}, force constant, is in mdyn/Å; R, equilibrium separation, is in Å; d_{AB}, parameters varying from 0.025 to 1.25 Å

for atoms through the third row. We take as an example O-H in H_2O and O···O in $(H_2O)_2$. R = 0.957 Å, d_{OH} = 0.335 Å giving K_{OH} = 7.7 mdyn/Å for O-H (experimental value, 7.8). Using Badger's covalent bond constant for second-row atoms, d_{AB} = 0.68, but the internuclear separation from the hydrogen-bonded water dimer, R = 3.0 Å, eq 3, yields K_{OO} = 0.15 mdyn/Å. Computed K_{OO} values are 0.18 for the Hartree-Fock AO basis,[18] 0.22 for the 4-31G basis with optimized geometry,[73] and 0.16 for an extended basis set including d polarization functions with optimized geometry.[73] The experimental value for ice[74] is 0.2 mdyn/Å. More generally, Badger's rule predicted K_{AB} range from 0.017 to 0.71 for $0.025 \leq d_{AB} \leq 1.25$ with the 36 computed R values.[16] This range of values is close to that obtained by direct calculation from the 36 dimer wave functions.[16] It is possible to propose a set of d_{AB} appropriate to the hydrogen bond. The principal accomplishment of Badger's rule is the good agreement with experiment obtained with parameters, d_{AB}, depending only on the rows of the atoms and, to be meaningful, hydrogen bond d_{AB}'s must be comparably simple.[75] The degree to which the lone pair of B overlaps A-H is the principal factor governing K_{AB}. For variable A-H, fixed B, lone-pair penetration is determined by μ_{A-H} and because R is inversely proportional to μ_{A-H}, the dependence of K_{AB} on A will be fully represented by variations in R, thereby making d_{AB} a constant for all A. For variable B, fixed A-H, lone-pair extent, l, is the principal variable. Because R is nearly constant for all B within a row, A-H overlap will be large for large l leading to large K_{AB}. Therefore, we expect d_{AB} to be proportional to l:

$$d_{AB} = d_B = l - \text{constant}$$

For the second row the constant is almost 0.8 Å. For the third row we recall that average l as a percent of average r is very close to that for the second row suggesting that to a first approximation d_B will depend only on its group in the periodic table. A set of values which satisfactorily order the 36 computed K_{AB} is:

	5	6	7
d_{AB}	1.00	0.80	0.55

(4)

Severe limitations on the accuracy of presently available data make further analysis unproductive.[76]

It is also useful to study additional features of the hydrogen-bond potential-energy surface as a function of R. Rather extended E_D vs. R curves have been computed for $(H_2O)_2$[77] and $(HF)_2$[78] and further knowledge of the curve shape has been obtained from fitting the Lippincott-Schroeder potential[79] to available experimental data. Qualitatively, the data suggest that the curves have the same general form and characteristics as those associated with ordinary bonds. This makes plausible the supposition that E_D is roughly proportional to K_{AB}.[80] A plot of 36 computed K_{AB} values against proton acceptors gives a set of six curves having a marked resemblance to Figure 1. Lack of experimental data and limitations in the available computed results put the search for an R, K_{AB}, E_D relationship outside of current capability.

K_{AH}. The accuracy of K_{AH} for the 36 dimers is low because the computations were carried out with fixed monomer geometries. A selected example that is hopefully representative of the $(K_{AH})_{dimer}/(K_{AH})_{monomer}$ dependence on BH_n is shown in Figure 18. ΔI is also plotted and the explanation of their parallel behavior is described schematically by the top part of Figure 19. The more I is lowered from its noble gas atom reference value, the greater the mixing between the A-H energy level and the energy level of B. Thus, for fixed A-H, electron-donor NH_3 perturbs and flattens out the proton well and lowers the force constant ratio to a greater degree than electron-donor FH. Third-row electron donors perturb the proton well less than second-row donors because their ionization potentials are lowered by a smaller amount from their noble gas reference atom and therefore the force constant ratio is lowered by a smaller amount. Rationalization of the change in K_{AH} with change in electron donor can be made in terms of I as well as ΔI. A plot of I vs. proton acceptors would parallel that of ΔI in Figure 18 and the longer I for NH_3 compared with FH clearly implies a greater perturbation of A-H.

The K_{AH} pattern for fixed BH_n, variable A-H, can likewise be understood in terms of model quantities (Figure 19, bottom). Enhancement of μ_{A-H} by charge redistribution parallels μ_{A-H} magnitudes. For a given row, the greater the buildup of negative charge on A (and the more positive H), the greater the lowering of $(K_{AH})_D/(K_{AH})_M$. Between rows approximate congener equality is anticipated because second- and third-row μ_{A-H} enhancements are approximately equal.[81]

G. Ir Intensity Enhancement and NMR Chemical Shift. One of the most distinguishing features of the hydrogen bond is the ir intensity enhancement

$$(\partial\mu/\partial r)_D^2/(\partial\mu/\partial r)_M^2$$

which accompanies its formation. The electronic structure origin of intensity enhancement is the charge redistribution produced by the new bond; charge transfer and augmentation of μ_{A-H} and of the BH_n dipole all increase the dimer dipole when an incremental change is made in r(A-H). Unfortunately, there have been no experimental measurements on gas phase dimers and little confidence can be placed in intensity enhancements computed from the available set of 36 dimer wave functions because experimental monomer geometries were employed. Qualitatively, however, the trends can be understood. As a first-order approximation, r(H···B) may be used instead of r(A-H) and numerical calculations show that variations in r(H···B) around equilibrium separation produces changes in CT, δ_A, and δ_{BL} roughly proportional to their equilibrium magnitudes. δ_A and δ_{BL} are indicative of μ_{A-H} enhancement and BH_n dipole enhancement, respectively. A plot of these and CT vs. BH_n (Figure 20) for a representative A-H (HS-H) is in accord with other reports[2] that CT contributed less than half of the observed ir intensity enhancement. Overall, we expect the intensity enhancement for electron-donor NH_3 to be greater than for FH, PH_3 greater than ClH, and the second row greater than the third because intensity enhancement qualitatively follows the charge rearrangement accompanying hydrogen-bond formation. The universal negative slopes for δ_{BL} vs. r(H···B) in all 36 dimers (Figure 21) are consistent with realization of an intensity enhancement. CT and δ_A vs. r(H···B) also show universal negative slopes and Figure 17, r(H···B) vs. μ_{A-H}, gives similar information.

The NMR chemical shift has proved to be a particularly useful experimental method for studying hydrogen bonding in the vapor phase[82] and in solutions and it would obviously be desirable to correlate properties of our model to the chemical shift. However, practical problems remain in obtaining hydrogen-bond chemical shifts from current quantum mechanical wave functions.[2] Thus, it may turn out that the properties of the present physical model can be related to the chemical shift, but at this time, there is insufficient knowledge and computational data to attempt a connection with model ideas.[83]

H. Alternative Models. The aspect of our model most open to question is the simple scheme used to estimate μ_{A-H} values. Calculation of dipole moments for individual molec-

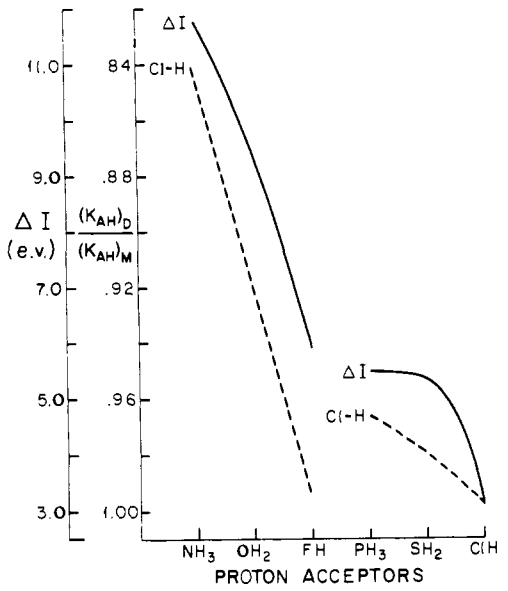

Figure 18. Proton donor force constant and ΔI vs. the six electron donors. (Solid line) ΔI for the six electron donors computed with 4-31G basis. (Dashed line) $(K_{Cl\text{-}H})_{dimer}/(K_{Cl\text{-}H})_{monomer}$ computed from dimer molecular orbital wave functions with the 4-31G basis.

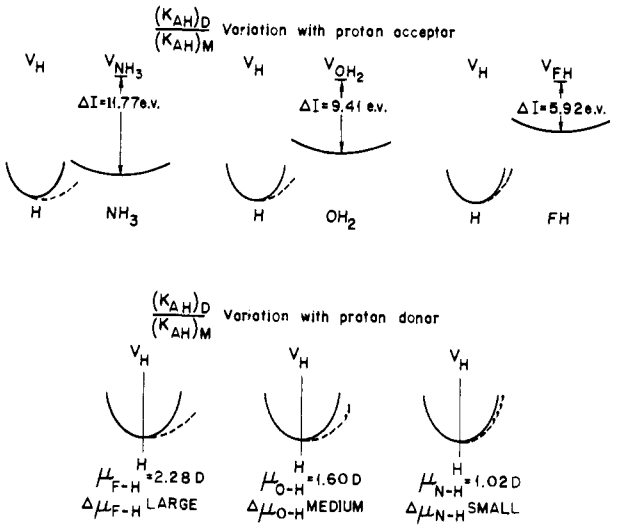

Figure 19. Schematic showing variation of proton donor force constants with change in electron donor (top) and with change in proton donor (bottom). Dashed lines represent change in hydrogen potential surface of monomer caused by electron donor (top) and by charge transfer and charge shift (bottom).

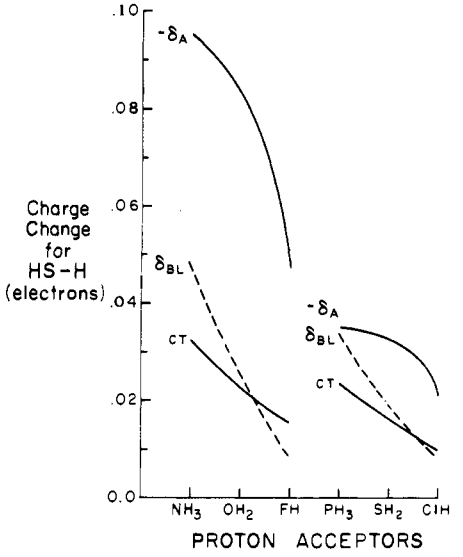

Figure 20. Charge transfer, charge change on proton donor A, and on hydrogens of electron donor for representative proton donor, HS-H, bonded to the six electron donors. Results from dimer molecular orbital wave functions with the 4-31G basis.

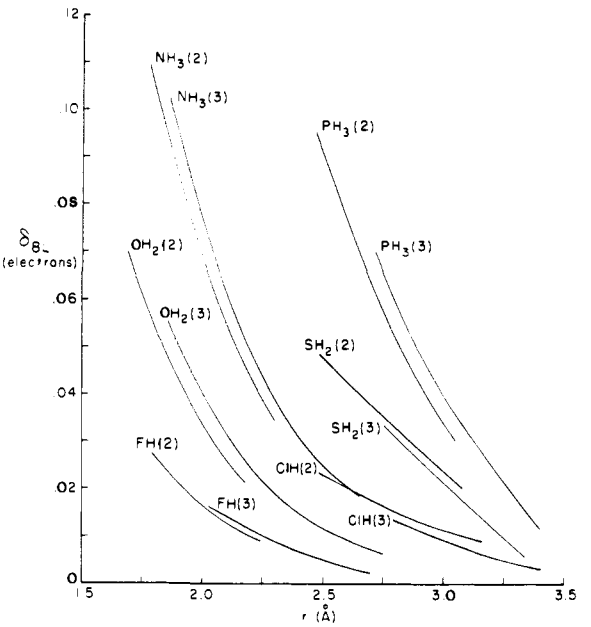

Figure 21. Charge change on electron-donor hydrogens for the six electron donors vs. r(H···B). Results from dimer molecular orbital wave functions with the 4-31G basis. (2) designates second-row proton donors and (3) designates third-row proton donors.

ular orbitals along with transformation and partitioning techniques could be suggested to obtain more detailed information on this quantity. It is also clear that a closer match to the available data could be obtained by introducing a different weighting factor for the symmetry axis lone pair in each of the six monomers. We do not pursue either of these possibilities because we believe the uncomplicated scheme employed provides an adequate introduction to the model and that further elaboration at this point would make it harder to evaluate its basis premises.

Another approach to the analysis of the available data is to use standard hybrids or localized orbitals obtained by transforming the canonical molecular orbitals.[84] Localized orbitals have the advantage that it is possible to compute the dipole operator expectation value for each electron pair bond separately thus determining $\mu_{A\text{-}H}$ directly from monomer wave functions. A disadvantage of this approach is the loss of Koopmans' theorem and therefore the simple connection between the highest-occupied electron-donor lone pair and the first ionization potential. Another disadvantage is that sp^3 hybridization and other directed bond schemes mix in s orbitals for B equal to O, F, S, and Cl and this does not appear necessary for understanding the properties of the 36 dimers to which our model is addressed.[85] Radial extents which include all electrons are not appreciably different than those employed here and it seems probable that the energy formula, eq 1, the stretching force formula eq 3, and the many other interrelationships shown by the current model likewise can be deduced from a localized orbital approach.

Other Hydrogen Bonds

In this part, we apply our model of the normal hydrogen bond to hydrogen bonds other than the 36 dimers from

Table XI. Parameters for Fourth Row Hydrides

BH_n	r(A–H), Å	μ, D	μ_{A-H}, D	I, eV	ΔI, eV	l,[h] Å
AsH_3	1.52[a]	0.20[a]	0.060	10.6[f]	3.40	2.37
SeH_2	1.46[b]	0.62[d]	0.33	9.88[f]	4.12	2.36
BrH	1.41[c]	0.82[e]	0.82	11.67[g]	2.33	2.14

[a] C. C. Loomis and M. W. P. Strandberg, *Phys. Rev.*, 81, 798 (1951). [b] A. W. Jache, P. W. Moser, and W. Gordy, *J. Chem. Phys.*, 25, 309 (1956). [c] L. E. Sutton, *Chem. Soc., Spec. Publ.*, No. 18 (1956–1959). [d] V. G. Veselago, *JETP Lett. (Engl. Trans.)*, 5, 513L (1957). [e] C. A. Burrus, *J. Chem. Phys.*, 31, 1270 (1959). [f] A. W. Potts and W. C. Price, *Proc. R. Soc. London, Ser A*, 326, 181 (1972). [g] H. J. Lempka, T. R. Passmore, and W. C. Price, *ibid.*, 304, 53 (1968), krypton first ionization potential is 14.00 eV. [h] Estimated from atomic wave functions.

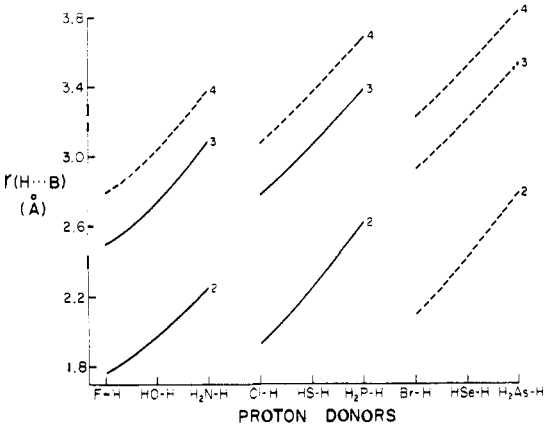

Figure 22. r(H···B) vs. proton donors of the second, third, and fourth rows. Solid lines: results from dimer molecular orbital wave functions with 4-31G basis. Dashed lines: extrapolation based on estimated fourth-row l values.

which it was derived. Most of our examples are gas phase dimers because a more detailed analysis of them is possible. Many fewer experimental and computational data are available than for the normal hydrogen-bonded dimers and in all cases research beyond the brief introduction given here will be required for full understanding.

A. Fourth-Row Hydrides. When AsH_3, SeH_2, and BrH are added to the collection of six monomers from the second and third rows 81 hydride dimers may be formed, 45 more than the original set of 36, and in this section we use the relationships from our model to predict their R and E_D. Experimental values for monomer first ionization potentials and dipole moments are available; ΔI and μ_{A-H} computed from these are given in Table XI. Since the atomic orbitals of the central atom undergo little distortion on hydride formation, l may be estimated from atomic 4p orbitals. In the second and third rows l is the radial distance at approximately 25% of the radial amplitude maximum. Applying this rule yields the l values in Table XI. Previously, we found that $\langle l_2\rangle/\langle l_2\rangle = \langle r_3\rangle/\langle r_2\rangle$, therefore $\langle r_4\rangle = \langle r_3\rangle(\langle l_4\rangle/\langle l_3\rangle) = (2.92)(1.10) = 3.2$ Å. The vertical separation between rows for a given proton donor is then obtained as $\langle r_4\rangle - \langle r_3\rangle = 0.3$ Å. The rule leading to constant r(H···B) per row for given A–H will be a good approximation for the fourth row and thus fourth row r(H···B) with second and third row A–H is easily obtained by a 0.3 Å vertical shift of the third-row curve as displayed by dashed lines in Figure 22. r(H···B) for fourth-row A–H is obtained by vertical displacement of the three third-row curves, but a rule analogous to the diagonal relationships is required to determine the vertical shift relative to the third row. Examining the various electronegativity scales, μ_{A-H}, and $1a_1$ vertical ionization potentials,[86] we find that neither a diagonal nor congener relationship holds exactly and we choose a reference half-way between (dashed lines, right side of Figure 22). Adding r(A–H) from Table XI to r(H···B) yields R, and E_D is then computed from eq 1. R and dimerization energies, referenced to $E_D = 7.0$ for the hydrogen fluoride dimer, are calculated in Table XII. An energy surface, Figure 23, has been constructed to provide a convenient method of visualizing interrelations among the dimer. Stretching force constants, K_{AB}, are expected to follow Badger's rule, eq 3, with the data in relation 4, and to show the parallelism with E_D found for the second and third row. K_{AB} trends are clear from this equation and the data in Table XII, but the level of precision currently available is too uncertain to present a numerical table. In a similar way, K_{AH} also should follow the pattern given for the second and third rows (Figure 19).

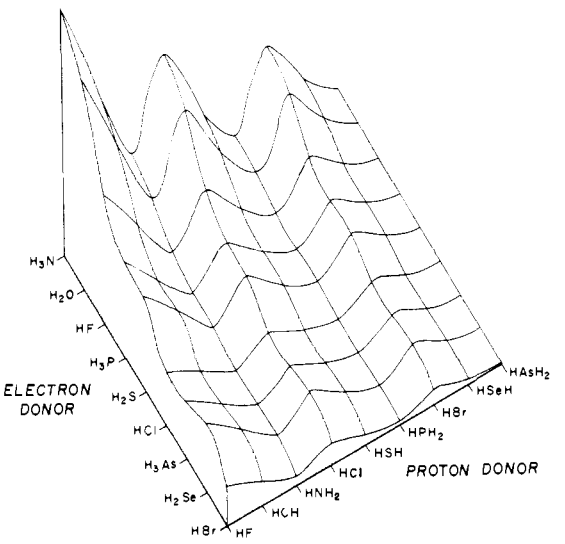

Figure 23. Dimerization energy surface for 81 dimers from second-, third-, and fourth-row monomers calculated by the E_D formula (eq 1). ΔI and μ_{A-H} derived from experimental ionization potentials and dipole moments. R from Figure 22 (Table XII).

B. Heteratomic Multiply Bonded Electron Donors. It often happens that the hydrogen-bonding electron-donor orbital is simultaneously involved in covalent bonding with monomer atoms rather than the pure lone pairs treated so far. Formaldehyde is an example and we compare it with water. Although no l value is available for formaldehyde and an ionization potential reference point is not obvious, it is to be expected that the effective ionization potential of oxygen and its relative polarizability will be roughly comparable to the oxygen in OH_2 because of the node between oxygen and carbon in its highest-occupied molecular orbital. The principal aspect differentiating formaldehyde from water is that its lone pair is distributed over four atoms. This difference will be reflected in the lone-pair charge in the hydrogen-bonding region and a measure of it is the ratio of the square of the monomer coefficients in the tails of the oxygen 2p orbitals: $(0.461/0.528)^2 = 0.76$. Calculations for F–H···OCH_2 with a 4-31G basis give $E_D = 10.0$ kcal/mol[17] compared with $E_D = 13.4$ kcal/mol for F–H···OH_2[16,17] yielding the ratio $10.0/13.4 = 0.75$.

Another effect in multiply bonded B is present in formamide. With proton donor F–H, 4-31G calculations yield a formamide E_D of 16.7 kcal/mol compared with 10.0 for formaldehyde.[17] The hydrogen bond is to the same σ orbital in the molecular plane as with formaldehyde. The additional feature in formamide is the well-known resonance

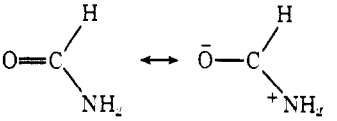

Table XII. Dimerization Energies[a] (kcal/mol) and Internuclear Separations[b] (Å) for Fourth-Row Hydrides

BH_n	F–H	HO–H	H_2N–H	Cl–H	HS–H	H_2P–H	Br–H	HSe–H	H_2As–H
R_2	2.68	2.93	3.26	3.19	3.57	4.03	3.50	3.88	4.31
NH_3	13.6	7.7	4.0	6.8	3.0	0.9	4.7	1.7	0.3
OH_2	11.4	6.5	3.4	5.7	2.5	0.8	3.9	1.4	0.2
FH	7.0	4.0	2.1	3.5	1.5	0.5	2.4	0.9	1.1
R_3	3.41	3.69	4.10	4.04	4.38	4.79	4.33	4.67	5.05
PH_3	5.2	3.0	1.6	2.6	1.2	0.4	1.8	0.7	0.1
SH_2	5.3	3.0	1.6	2.7	1.2	0.4	1.9	0.7	0.1
ClH	3.0	1.7	0.9	1.5	0.7	0.2	1.1	0.4	0.1
R_4	3.71	3.99	4.40	4.34	4.68	5.09	4.63	4.97	5.35
AsH_3	3.1	1.8	1.0	1.6	0.7	0.2	1.1	0.4	0.1
SeH_2	3.8	2.2	1.2	1.9	0.9	0.3	1.4	0.5	0.1
BrH	2.1	1.2	0.7	1.1	0.5	0.2	0.8	0.3	0.1

[a] Computed from eq 1 using data from Table XI. $K = 1.87$ set by choosing $E_D = 7.0$ for $(FH)_2$. [b] R_j are $R(A\cdots B)$ averaged over j^{th} row of the periodic table.

which builds up a sizable charge in the π orbital perpendicular to the plane of the hydrogen bond. Symmetry prevents mixing of this π orbital with the hydrogen-bonding molecular orbitals, but it has two other effects that differentiate it from formaldehyde. First, its added electron repulsion pushes some charge out of the oxygen $2p\sigma$, slightly reducing the hydrogen-bond strength. Second, the significantly enhanced charge on oxygen makes an electrostatic contribution that is nearly half the dimerization energy. The nature of this effect is analyzed more completely in section F.

C. Weak Hydrogen Bonds. Another class of multiply bonded electron donors are the double and triple bonds between carbon atoms and conjugated hydrocarbons. These give rise to weak or π hydrogen bonds and their dimerization energies are roughly one-fifth the magnitude of a corresponding pure lone pair. As an illustration, we compare ethylene with acetylene for proton donor F-H. The F-H internuclear axis is perpendicular to the C-C axis and pointed at a carbon atom. Calculations carried out with the 4-31G basis find E_D equal to 2.9 and 2.5 kcal/mol, respectively, and the same R for both.[17] In this case an approximate ionization potential reference can easily be established and eq 1 employed. The highest occupied MO is spread over two centers, but we assume it to be a superposition of two independent π orbitals and take neon as reference. $\Delta I = 21.56 - 10.51^{87} = 11.05$ eV and $21.56 - 11.40^{87} = 10.16$ eV for ethylene and acetylene, respectively, yielding the ratio $11.05/10.16 = 1.09$ compared to the quantum mechanically determined dimerization energy ratio, $2.9/2.5 = 1.16$. If F-H is pointed at the center of the π bond rather than toward a carbon, a considerable increase in both E_D is anticipated because of the charge increase resulting from overlap of the $2p\pi$ orbitals and the calculations bear this out.

Another test of eq 1 with ethylene and acetylene as electron donors is possible by changing proton donors. Del Bene, using a simpler basis (STO-3G) then 4-31G, has made calculations for the center of the π bond with proton donors F-H and HO-H.[88] For a given electron donor, the ratio of E_D times R should equal $\mu_{F\text{-}H}/\mu_{O\text{-}H}$. Her computations yield 1.38 and 1.26 for ethylene and acetylene, respectively. $\mu_{F\text{-}H}/\mu_{O\text{-}H}$ obtained from STO-3G dipole moments (FH, 1.29; OH_2, 1.69)[89] is $1.29/1.03 = 1.25$.

D. Substitution at B. Calculations at STO-3G have been made for electron-donors OHX where X = H, CH_3, NH_2, OH, and F with proton-donor HO-H.[90] Some of the nonhydride bonds can mix with the oxygen $2p\pi$ and the distortion produced by these bonds prevents a monotonic relation between the first ionization potential and lone-pair energy lowering. For hydrogen bonding, the principal action of the substituent is withdrawal of charge from O and a reasonable approach for the case of these single bonded substituents is to assume I proportional to the charge on oxygen. Therefore, we connect oxygen charge[90] linearly with calculated $(E_D)(R)$ and the predicted E_D compared to direct calculations (in parentheses)[90] are: OH_2, 6.0 kcal/mol (5.9); $OHCH_3$, 5.1 (5.2); $OHNH_2$, 4.0 (4.0); OHOH, 3.3 (3.4); OHF, 2.6 (2.8). In her article, Del Bene recognized the direct relationship between oxygen charge and hydrogen-bond strength and suggested this charge as an approximate indicator of dimerization energy.

E. Hydrogen-Bonded Polymers. In extending our model from dimers to trimers we use the energy reference property of ΔI to predict trimer energies from dimer and monomer quantities. Our results apply only to an optimally positioned trimer. Equation 1 shows that:

$$E_{dimer} \sim \Delta I(\text{monomer}) \equiv I_{atom} - I_{monomer} \qquad (5)$$

If R is assumed to be the same for the dimer and trimer and if we are dealing with a single type of monomer, then

$$E_{trimer} - E_{dimer} \sim \Delta I(\text{dimer}) - \Delta I(\text{monomer}) = I_{monomer} - I_{dimer} \qquad (6)$$

From eq 5 we can obtain the scale factor between E_{dimer} and ΔI(monomer) and use it in eq 6 to predict the nonadditivity energy. The formation of a dimer is accompanied by charge transfer from electron donor to proton donor A and this additional charge raises the potential around A, slightly lowering the ionization potential of that A lone pair which will become the hydrogen-bonding lone pair for the new bond in the trimer. The increased ΔI results in the greater stability for the trimer over that of two isolated dimers. 4-31G calculations[16] on $(HF)_2$ yield $E_{dimer} = 7.87$ kcal/mol., ΔI(monomer) = 5.92 eV, $I_{monomer} - I_{dimer} = 0.975$ eV, and consequently $E_{trimer} - E_{dimer} = 1.3$ kcal/bond nonadditivity. Del Bene and Pople,[91] employing an STO basis, have made a direct computation of the nonadditivity with $R_{trimer} = R_{dimer}$ and obtained 1.15 kcal/bond. Similar results for H_2O monomer are $E_{trimer} - E_{dimer} = 0.95$ kcal/bond from $I_{monomer} - I_{dimer}$ and 1.05 kcal/bond from direct computation.[92] Hankins *et al.*[14] using an extended basis find 0.71 kcal/bond by direct computation. For $(H_2O)_3$, Del Bene and Pople[92] find a 3.5% reduction in R compared to the dimer but this is so small that it is not worthwhile correcting for the R ratio. No direct computations are currently available for other polymers, but predictions can be easily made from calculated monomer and dimer ionization potentials and they show an interesting pattern. For $(NH_3)_3$ nonadditivity is 0.33 kcal/bond. For third-row monomers nonadditivity is an order of magnitude less, a notably larger reduction than might be presumed from dimerization energy ratios, but it follows the same order, ClH > SH_2 > PH_3, and relative spread found for the second row. The explanation of nonadditivity suggested by our model also implies, in

principle, the possibility of a lower energy cyclic structure because the final link has the potential benefit of a slightly lowered I not realized by the open polymer. It should be noted that the estimation procedure given in this section is analogous to first-order perturbation theory and does not take into account the charge redistribution occurring when a trimer is made from a dimer and this means that properties such as polymer dipole moment, geometry, and successive nonadditivity effects are outside its domain.

F. Strong Hydrogen Bonds. The physical properties of strong hydrogen bonds are sufficiently different from normal and weak hydrogen bonds that sometimes they have been classified with ionic covalent bonds, thus they present a severe challenge to our model. As in the section above, we are attempting to extend the model into a new domain and again we need the energy reference provided by ΔI in eq 1. Extended basis calculations for $F^-\cdots H\text{-}OH$ and $Cl^-\cdots H\text{-}OH$ are available[93] and according to eq 1 the E_D ratio for these two systems should be:

$$E_D(F^-)/E_D(Cl^-) = (\Delta I_{F^-}/\Delta I_{Cl^-})(R_{Cl^-}/R_{F^-})$$

Experimental electron affinities for F and Cl are 3.50 and 3.62 eV, respectively,[94] giving $\Delta I_{F^-} = 18.06$ and $\Delta I_{Cl^-} = 12.13$. Computed internuclear separations and dimerization energies are 2.51 and 3.31 Å and 23.54 and 11.86 kcal/mol for the fluorine and chlorine dimers, respectively. Therefore the ratio predicted from the model is (18.06)(3.31)/(12.13)(2.51) = 1.96 compared to (23.54)/(11.86) = 1.98. We now attempt an absolute determination of E_D from eq 1 and, since the evaluation above shows that ΔI is successfully representing the electron donor, this will reveal what is taking place on the proton donor. Kraemer and Diercksen[95] have carried out a computation for $F^-\cdots H\text{-}OH$ with an extended basis of essentially identical quality to that of Kistenmacher et al.,[93] and for current purposes, it has the advantage that Diercksen et al.[20] have performed four parallel calculations on normal hydrogen bonds and using their E_D and R for $(H_2O)_2$ sets the energy scale factor and eliminates the dependence on $\mu_{A\text{-}H}$, thus:

$$E_D(F^-HOH) = E_D(H_2OHOH)(R_{OO})(\Delta I_{F^-})/(R_{FO})(\Delta I_{OH_2}) = (4.84)(3.0)(18.06)/(2.51)(8.94) = 11.69 \text{ kcal/mol}$$

compared to $E_D = 22.07$ kcal/mol computed from the wave function (with fixed monomer geometry for H_2O), showing that eq 1 is yielding approximately 50% of the dimerization energy. The additional binding energy is due to the direct Coulomb attraction between F^- and the positive hydrogen and increased charge shift on H-OH. The internuclear separation is smaller than normal hydrogen bonds, F^- pushes charge off H onto O, and the hydrogen-bonding electron pair supplied by F^- overlaps H-OH to a greater extent, raising E_D. Application of Clementi's bond energy analysis to this dimer by Kistenmacher et al.[93] supports this interpretation. $(FHF)^-$ represents an extreme case with the hydrogen midway between the heavy atoms and the internuclear separation still smaller than $F^-\cdots H\text{-}OH$.[96] If we write this bond as $F^-\cdots H\text{-}F$ and ignore proton movement we can again compare our normal bond energy formula with results from a high-accuracy quantum calculation. Noble and Kortzeborn[97] have computed an $(FHF)^-$ wave function from an extended basis similar to those employed by Diercksen and, again using Diercksen's normal hydrogen bond results[20] ($(FH)_2$ in this case) to calibrate the E_D formula and eliminate dependence on $\mu_{F\text{-}H}$, the dissociation energy is given by eq 1 as:

$$E_D(FHF)^- = E_D(HF)_2(R_{FF})(\Delta I_{F^-})/(R_{FHF^-})(\Delta I_{FH}) = (4.5)(2.85)(18.06)/(2.25)(5.51) = 18.68 \text{ kcal/mol}$$

The experimental value[98] and that computed by Noble and Kortzeborn[97] are $R = 2.27$ Å, $E_D = 37$ kcal/mol; $R = 2.25$ Å, $E_D = 40.24$ kcal/mol, respectively, again showing that eq 1 yields approximately 50% of the observed E_D for strong hydrogen bonds. The ability of $\Delta I/R$ to represent the electron-donor energetics for strong negative ion hydrogen bonds and the bond energy analysis of Kistenmacher et al.[93] suggest that the energy formula for normal bonds may be extended by adding a Coulomb term. Assuming $B^-\cdots H\text{-}A$ as a representation of strong negative ion hydrogen bonds, the potential at H due to the negative charge on B is $1/r$ where r is $r(H\cdots B)$. The charge on H may be taken proportional to $\mu_{A\text{-}H}$ to a good approximation and therefore the energy lowering at H due to the Coulomb potential is (constant)$K\mu_{A\text{-}H}/r$ where K, the energy scale factor, can be absorbed in the constant. If we chose ten as a rough first approximation for the constant, the strong bond energy formula is

$$E_D = K\mu_{A\text{-}H}(\Delta I/R + 10/r) \quad (7)$$

Equation 7 accounts for the greater charge shift on A-H because this is expected to be proportional to $\mu_{A\text{-}H}$ as it is in normal hydrogen bonds. Calculations with optimized r(A-H) and R have been carried out for four systems and fortunately these cover a large part of the range expected for strong hydrogen bonds. The available systems and internuclear separations are: $F^-\cdots H\text{-}OH$,[95] $r = 1.50$ Å, $R = 2.51$ Å; $Cl^-\cdots H\text{-}OH$,[93] $r = 2.35$, $R = 3.31$; $(FHF)^-$, $r = 1.125$, $R = 2.25$;[97] $(HOHOH)^-$, $r = 1.21$, $R = 2.41$.[99] Using Diercksen et al.[20] normal bond calculations on $(H_2O)_2$ and $(HF)_2$ to set the energy scale factor, E_D values from eq 7 compared to the direct calculations (parentheses) are: $F^-\cdots H\text{-}OH$, 22.5 kcal/mol (24.07[95] and 23.54[93]); $Cl^-\cdots H\text{-}OH$, 12.8 (11.86); $(FHF)^-$, 39.4 (40.24); $(HOHOH)^-$, 27.3 (31.8). The traditional example of strong positive ion hydrogen bonds is symmetrical $(H_5O_2)^+$. If we write this as

$$H_2O^+\text{-}H\cdots OH_2$$

it suggests enhanced $\mu_{A\text{-}H}$ as the origin of strong bonding and leads to an energy formula

$$E_D = K(\mu_{A\text{-}H} + D)\Delta I/R \quad (8)$$

where D is the dipole moment lying along the same line as $\mu_{A\text{-}H}$ that results from the positive charge. Unfortunately, data are too scarce to check eq 8. Equations 7 and 8 ignore the considerable proton shift from its monomer position. In symmetrical $(FHF)^-$ this shift is 23%. It may be that the increase in the covalent contribution between electron donor and the hydrogen is cancelled by the decrease in covalent contribution in the A-H bond.

Noble and Kortzeborn[97] also carried out a calculation on the free atom-diatomic interaction, $F\cdots H\text{-}F$, finding $R = 3.03$ Å and $E_D = 3.0$ kcal/mol. With the same calibration from Diercksen employed above plus $\Delta I_F = 21.56 - 17.42 = 4.14$ eV from experiment, eq 1 gives:

$$E_D(F\cdots H\text{-}F) = (4.5)(2.85)(4.14)/(3.03)(5.51) = 3.2 \text{ kcal/mol}$$

The success of eq 1 for the free atom-diatomic molecule hydrogen bond indicates that this interaction is of the same nature as other normal hydrogen bonds and it also illustrates the ability of the model to encompass a very broad range of hydrogen-bonding phenomena. In addition to $F\cdots H\text{-}F$, there has been considerable recent interest in the hydrogen dichloride radical and higher dihalide radicals.[100]

$\Delta I_{Cl} = 15.76 - 12.97 = 2.79$ eV and using eq 1 along with any reasonable R leads to an E_D roughly half that of F···H-F. The experiment, on the other hand,[100] suggests an E_D comparable to the ion $(ClHCl)^-$ and a symmetrical, $D_{\infty h}$, structure. The symmetrical hydrogen difluoride radical has been found unbound (barrier height approximately 18 kcal/mol) by two independent, quite sophisticated ab initio calculations,[97,101] but chlorine may act differently than fluorine. In Cl-H···NH_3, ab initio calculations[16,102] have shown that the hydrogen drifts toward a center position, but does not appreciably drift in F-H···NH_3, and ΔI for Cl is close to ΔI for ClH but this is not true for F and FH. These observations along with the above E_D estimate for asymmetrical Cl···H-Cl imply that symmetrical ClHCl could be bound by 1.5 kcal/mol or more[103] and points to the need for a high-quality ab initio calculation for this radical.

G. Substitution at and for A. When proton-donor substitutions are made a problem arises when more than one electronegative atom is substituted for A. In this situation the component of the monomer dipole moment along A-H is generally too large because long distances are involved and the extra atoms are further from the H···B region, thus exerting a lesser influence on hydrogen-bond formation. One way to solve this problem is use of electrostatic potentials to represent μ_{A-H} as discussed in a previous section. Another crude but satisfactory method for illustrating the workings of the model is to employ the hydrogen charge on the monomer determined by population analysis. The greater the electronegativity of the proton donor, the more positive the hydrogen-bonding hydrogen is expected to be and therefore we assume μ_{A-H} proportional to q_H for a given class of proton donors. As a test we examine μ_{A-H} and q_H for the monomers, F-H, $q_H = +0.48$; HO-H, +0.39; H_2N-H, +0.30, calculated at 4-31G. q_H vs. μ_{A-H} is quite close to a straight line. q_H vs. μ_{A-H} for the third-row monomers, Cl-H, HS-H, H_2P-H, is almost linear with the same slope.

Two sets of dimer wave functions exist in the literature which treat a wide variety of proton donors. Del Bene[104] has made computations at STO-3G for XO-H···NH_3, XO-H···OH_2, and XO-H···OCH_2 with X = H, CH_3, NH_2, OH, and F. Kollman et al.[17] have computed dimers at 4-31G for electron-donor NH_3 with proton-donors H_3C-H, F_3C-H, PC-H, H_2CN-H, NC-H, and CN-H. For proton donors studied by Del Bene, μ_{A-H} will be ordered according to FO-H, OHO-H, NH_2O-H, CH_3O-H, HO-H. Thus we expect, and find, that $(E_D)(R)$ has this same order for each of the three electron donors. The assumption of μ_{A-H} proportional to q_H gives μ_{A-H} values which are equally spaced.[105] According to eq 1 therefore a plot of $(E_d)(R)$ vs. equally spaced XO-H should produce straight lines. The resultant E_D from the linear fit compared to computed values (parentheses) in the order HO-H, CH_3O-H, NH_3O-H, OHO-H, FO-H are: for NH_3, 5.6 (5.9), 6.6 (6.5), 7.5 (7.1), 8.4 (8.0), 9.2 (9.8); for OH_2, 5.7 (5.9), 6.5 (6.3), 7.2 (7.3), 7.8 (7.6), 8.4 (8.7); for OCH_2, 3.1 (3.3), 3.6 (3.5), 4.1 (4.2), 4.5 (4.4), 4.9 (5.0). Finer grained examination of the $(E_D)(R)$ vs. XO-H shows a systematic alternation of values above and below the straight lines for each electron donor indicating that X = CH_3 should be closer to X = H and X = OH should be closer to X = NH_2. These shifts are in accord with what is expected from electronegativity considerations.

The proton donor set computed by Kollman et al.[17] can be analyzed by the same rough approximation. Thus if $(E_D)(R)$ is assumed proportional to q_H and a line is fitted to the highest and lowest values, E_D are: 1.1 (1.1), 3.4 (7.6), 4.8 (4.6), 6.8 (5.5), 8.0 (9.7), 13.1 (13.1). Proton-donor F_3C-H is out of order and it is clear why this occurs: there is a large electronegativity difference between F and C, charge is transferred from C to F building up a sizable bond dipole, but a considerably lesser amount is withdrawn from H by C.

Summary

Using definitions based on the molecular orbital representation, we have established three monomer quantities: μ_{A-H}, ΔI, and l, which characterize a physical model of the normal hydrogen bond. This model organizes results computed from ab initio wave functions and rationalizes the dimerization energy, charge transfer, dipole moment, internuclear separation, directionality, stretching force constants, and ir intensity enhancement.

(1) Dimerization energy can be expressed as

$$E_D = K\mu_{A-H}\Delta I/R$$

This formula is able to match all sets of ab initio wave functions, existing experimental measurements, and the electrostatic potential calculations. For each row, a nearly linear relationship exists between ΔI and l and this is helpful in extending the dimerization energy formula to complex electron donors where an ionization potential reference point is not apparent. The tendency for strong bonding electron donors to be weak bonding proton donors, and vice versa, is the result of a reciprocal relation between μ_{A-H} and ΔI (or l) which is intrinsic to a monomer. Since these quantities appear linearly in the E_D formula qualitative reasoning is aided on such questions as which of two monomers will be the proton donor and which electron donor for the lowest energy dimer.

(2) Charge transfer is nearly proportional to μ_{A-H} for specified B and ordered according to l within a row for specified A. Charge transfer is similar for second- and third-row electron donors because average l as a percent of average r(H···B) is nearly the same for both rows. Charge change on the electron donor, δ_{BL}, is linear in μ_{A-H}, extrapolating to zero for zero μ_{A-H}, thus revealing μ_{A-H} as the driving force for this charge rearrangement. For specified A, charge accumulation on the proton donor is ordered by l. The electron donor charge change, δ_{BL}, extrapolates to zero at neon for second-row B and argon for third-row B, thus substantiating the noble gas atoms as appropriate ionization potential reference points.

(3) Dimer dipole moments parallel μ_{A-H}. Moments for third-row electron donors are smaller than the second row because bond angles are larger.

(4) The hydrogen-bond length, r(H···B), is inversely proportional to μ_{A-H} and nearly independent of B for a given row. The origin of this independence is found in the constancy of l times I. Because changes in r are almost independent of B within a row, r vs. μ_{A-H} closely resembles two parallel lines. Between rows, the ratio of average r(H···B) is almost exactly equal to the corresponding ratio of average l values.

(5) Directionality is a competition between the angular charge distribution of the lone pairs and the dipole-dipole interaction between the proton donor and electron donor with electron donors NH_3 and PH_3 always leading to $\theta = 0°$. For fixed B, θ is inversely related to μ_{A-H}. For fixed A, θ is inversely related to electron donor dipole moment; third-row B have smaller dipole moments and notably larger θ than second-row B.

(6) Stretching force constants K_{AB} follow Badger's rule

$$K_{AB}(R - d_{AB})^3 = 1.86$$

with d_{AB} independent of the row and equal to 1.00, 0.80, and 0.55 for groups 5, 6, 7, respectively. Relative to the proton-donor monomer, K_{AH} is inversely proportional to μ_{A-H}

for given B and inversely proportional to ΔI (or I) for given A-H.

(7) Augmentation of μ_{A-H} and the electron donor dipole moment by the charge redistribution on dimer formation is the cause of a significant infrared intensity enhancement for all hydrogen bonds. The enhancement parallels charge transfer and is expected to be ordered according to I within a row for specified A. The model is also successful in rationalizing properties of other hydrogen bonds.

(a) For fourth-row hydride monomers an estimate of I can be obtained from atoms and r from average I. When taken together with spectroscopic data on I and μ, this leads to quantitative prediction of E_D for dimers formed with fourth-row monomers.

(b) The weak hydrogen bonds formed with the π bonds of organic molecules can also be understood with the dimerization energy formula. Ethylene and acetylene are examples. Neon can be used as an approximate ionization potential reference and satisfactory agreement with ab initio dimer calculations was obtained for these electron donors.

(c) For multiply bonded, heteratomic electron donors the charge distribution of the electron-donor lone pair is a principal factor. Formaldehyde is an example and it was found that diminished charge in the hydrogen-bonding region could explain its energetics compared to that of water. In formamide, the amide resonance gives rise to an added ionic contribution similar to that found in strong hydrogen bonds.

(d) When an electronegative substituent replaces hydrogen on a hydride electron donor the change in I may be approximated by the change in the charge on B. E_D obtained by this scheme agreed well with ab initio dimer computations for substituents CH_3, NH_2, OH, and F.

(e) For homogeneous hydrogen-bonded polymers, the dissociation energy nonadditivity in going from a dimer to an optimally positioned trimer was shown to be proportional to:

$$I_{\text{monomer}} - I_{\text{dimer}}$$

and is always positive. A similar argument can be made in contrasting open to cyclic systems and therefore a cyclic structure will be the more stable if all other conditions are equal.

(f) The ratio of computed dimerization energies between $F^-\cdots H\text{-}OH$ and $Cl^-\cdots H\text{-}OH$ and between $F\cdots H\text{-}F$ and $HF\cdots H\text{-}F$ shows good agreement with corresponding ΔI ratios, thereby supporting the meaningfulness of the model beyond the range of the normal hydrogen bonds.

(g) Qualitative understanding of the large dissociation energies found in the extreme examples of strong hydrogen bonds, $(FHF)^-$ and $(H_5O_2)^+$, can be obtained by recalling their small R values and writing their structures as normal hydrogen bonds:

$$F^-\cdots H\text{-}F \quad \text{and} \quad H_2O^+\text{-}H\cdots OH_2$$

thus pictorially demonstrating the increase in binding energy due to ΔI or I increase or μ_{A-H} increase, respectively. Chemically useful dissociation energy estimates for strong negative ion hydrogen bonds can be obtained by adding a Coulomb term to the dimerization energy expression resulting in the formula,

$$E_D = K\mu_{A-H}(\Delta I/R + 10/r)$$

(h) Substitutions for A imply changes in μ_{A-H} and these can be understood qualitatively by the approximate proportionality between μ_{A-H} and monomer q_H. Substituents with a wide variety of bonding structures are ordered by this scheme and deviations from this order are also readily explained.

Acknowledgment. The author thanks William C. Topp, Robert Belkin, and Philip W. Payne for their sustained and conscientious efforts in calculating dipole-dipole energies, nonequilibrium R dimers, and I values and for useful general comments. He thanks Peter A. Kollman for enlightening criticism and stimulating discussion. He also wishes to acknowledge generous financial support from the Molecular Biology Section of the National Science Foundation.

References and Notes

(1) D. Hadzi and W. H. Thompson, Ed., "Hydrogen Bonding", Pergamon Press, Oxford, 1959; G. C. Pimentel and A. L. McClellan, "The Hydrogen Bond", W. H. Freeman, San Francisco, Calif., 1960; N. D. Sokolov and V. M. Tschulanovskü, Ed., "Vodorondnaya Svyaz", Nauka, Moscow, 1964; W. C. Hamilton and J. Ibers, "Hydrogen Bonding in Solids", W. A. Benjamin, New York, N.Y., 1968; S. N. Vinogradov and R. H. Linnell, "Hydrogen Bonding", Van Nostrand-Reinhold, New York, N.Y., 1971; M. D. Joesten and L. J. Schaad, "Hydrogen Bonding", Marcel Dekker, New York, N.Y., 1974; this latter book gives a complete literature tabulation 1960–1973 inclusive.

(2) C. N. R. Rao, in "Water, A Comprehensive Treatise", Vol. 1, Felix Franks, Ed., Plenum Press, New York, N.Y., 1972, Chapter 3; P. A. Kollman and L. C. Allen, *Chem. Rev.*, **72**, 283 (1972); G. C. Pimentel and A. L. McClellan, *Annu. Rev. Phys. Chem.*, **22**, 347 (1971). These latter two reviews give a list of all previous reviews. In Chapter 2 of the most recent book (ref 1), Schaad gives a very thorough, critical review of theoretical methods and results with special attention to $(H_2O)_2$ and $(FHF)^-$.

(3) S. Bratoz, *Adv. Quantum Chem.*, **3**, 209 (1967); H. Ratajczak, *J. Phys. Chem.*, **76**, 3000 (1972).

(4) R. S. Mulliken, *J. Am. Chem. Soc.*, **74**, 811 (1952); *J. Phys. Chem.*, **56**, 801 (1952); R. S. Mulliken and W. B. Person, *Annu. Rev. Phys. Chem.*, **13**, 107 (1962).

(5) C. A. Coulson, *Res. Appl. Ind.*, **10**, 149 (1957).

(6) G. C. Pimentel, *J. Chem. Phys.*, **19**, 446 (1951); see also the description in Chapter 8 of his book (ref 1).

(7) H. Bethe, *Ann. Phys. (Leipzig)*, **3**, 143 (1929).

(8) See L. Pauling, "The Nature of the Chemical Bond", 3rd ed, Cornell University Press, Ithaca, N.Y., 1960, Chapter 13.

(9) G. N. Lewis, *J. Am. Chem. Soc.*, **38**, 762 (1916); W. Kossel, *Ann. Phys. (Leipzig)*, **49**, 229 (1916).

(10) F. London, *Z. Phys.*, **63**, 245 (1930); *Z. Phys. Chem., Abt. B*, **11**, 222 (1930).

(11) M. Goeppert-Mayer and J. H. D. Jensen, "Elementary Theory of Nuclear Shell Structure", Wiley, New York, N.Y., 1955.

(12) See C. Kittel, "Introduction to Solid State Physics", 4th ed, Wiley, New York, N.Y., 1971, Chapter 10.

(13) R. Hoffmann, *Chem. Eng. News*, **52**, 32 (July 29, 1974).

(14) H. Popkie, H. Kistenmacher, and E. Clementi, *J. Chem. Phys.*, **59**, 1325 (1973); D. Hankins, J. W. Moskowitz, and F. H. Stillinger, *Ibid.*, **53**, 4544 (1970); G. H. D. Diercksen, *Theor. Chim. Acta*, **21**, 335 (1971); L. A. Curtiss and J. A. Pople, *J. Mol. Spectrosc.*, **48**, 413 (1973); *J. Chem. Phys.*, in press.

(15) H. Popkie, H. Kistenmacher, and E. Clementi, *J. Chem. Phys.*, **59**, 1325 (1973); A. Meunier, B. Levy, and J. Berthier, *Theor. Chim. Acta*, **29**, 49 (1973); D. Hankins, J. W. Moskowitz, and F. H. Stillinger, *J. Chem. Phys.*, **53**, 4544 (1970); G. F. H. Diercksen, W. P. Kraemer, and B. O. Roos, *Theor. Chim. Acta*, **36**, 249 (1975). It is suggested in this article that the correlation correction may be almost cancelled by zero-point energy corrections: O. Matsuoka, E. Clementi, and M. Yoshimine, to be published.

(16) W. C. Topp and L. C. Allen, *J. Am. Chem. Soc.*, **96**, 5291 (1974). Monomer geometries are: NH_3, r(N–H) = 1.014 Å, α = 107.05°; OH_2, r(O–H) = 0.957 Å, α = 104.52°; FH, r(F–H) = 0.917 Å; PH_3, r(P–H) = 1.41 Å, α = 93.8°; SH_2, r(S–H) = 1.32 Å, α = 92.2°; ClH, r(Cl–H) = 1.27 Å.

(17) P. A. Kollman, J. McKelvery, A. Johansson, and S. Rothenberg, *J. Am. Chem. Soc.*, **97**, 955 (1975).

(18) P. A. Kollman and L. C. Allen, *J. Am. Chem. Soc.*, **93**, 4991 (1971).

(19) J. Dill, W. C. Topp, L. C. Allen, and J. A. Pople, *J. Am. Chem. Soc.*, in press.

(20) G. H. F. Diercksen, *Chem. Phys. Lett.*, **4**, 373 (1970); *Theor. Chim. Acta*, **21**, 335 (1971); G. H. F. Diercksen and W. P. Kraemer, *Chem. Phys. Lett.*, **6**, 419 (1970); G. H. F. Diercksen, W. P. Kraemer, and W. von Niessen, *Theor. Chim. Acta*, **28**, 67 (1972).

(21) S. Rothenberg, R. H. Young, and H. F. Schaefer III, *J. Am. Chem. Soc.*, **92**, 3243 (1970). Compare hydrides in this paper with SO_2 in S. Rothenberg and H. F. Schaefer III, *J. Chem. Phys.*, **53**, 3014 (1970).

(22) D. G. Cooper, "The Periodic Table", 3rd ed, Butterworths, London, 1964, pp 68–76.

(23) F. A. Cotton and G. Wilkinson, "Advanced Inorganic Chemistry", 3rd ed, Wiley-Interscience, New York, N.Y., 1972; M. C. Day and K. Selbin, "Theoretical Inorganic Chemistry", 2nd ed, Reinhold, New York, N.Y., 1969; R. T. Sanderson, "Chemical Bonds and Bond Energies", Academic Press, New York, N.Y., 1971; B. E. Douglas and D. H. McDaniel, "Concepts and Models of Inorganic Chemistry", Blaisdell-Ginn, New York, N.Y., 1965.

(24) The possibility of averaging congener r values, F–H with Cl–H, H–OH with HS–H, and H_2N–H with H_2P–H might be proposed, but the r differ-

ences are large and simple patterns and trends are mostly destroyed.
(25) B. Katz, A. Ron, and O. Schnepp, *J. Chem. Phys.*, **47**, 5303 (1967); C. Girardet and D. Robert, *ibid.*, **58**, 4410 (1973).
(26) P. A. Kollman, J. McKelvey, A. Johansson, and S. Rothenberg, *J. Am. Chem. Soc.*, **97**, 955 (1975); W. C. Topp and L. C. Allen, to be published.
(27) Consideration of orbital overlaps and hydrogen-bond charge shifts suggest this as an appropriate measure, but other choices preserve relative values as well as the properties attributed to I values. For OH_2, e.g., 90% enclosed charge leads to $I = 1.18$ Å and 99% to 1.72 Å.
(28) L. Pauling, "The Nature of the Chemical Bond", 3rd ed, Cornell University Press, Ithaca, N.Y., 1960, Chapter 7.
(29) Figure 7 is taken from R. J. Buenker and S. D. Peyerimhoff, *Chem. Rev.*, **74**, 174 (1974). Charge density contours for other monomers are given in D. B. Boyd, *J. Chem. Phys.*, **52**, 4846 (1970).
(30) In perturbation theory, the energy through first order may be obtained from the unperturbed wave functions.
(31) Several important recent papers have provided striking numerical confirmation of this reference choice. M. Losonczy, J. W. Moskowitz, and F. H. Stillinger, *J. Chem. Phys.*, **59**, 3264 (1973); *ibid.*, in press, have carried out extended basis molecular orbital calculations on Ne···H–OH, Ar···H–OH, and Ne···H–F. The E_D values are 0.17, 0.02, and 0.234 kcal/mol, respectively. These values are of the same order as London dispersion energies. Dimerization energies for NeHOH and NeHF are both 15 times smaller than dimers with the same proton donor and the electron donor of lowest E_D (HClHOH, HClHF) and represent energies separated from our dimer E_D values by an amount that is several times greater than the full spread of dissociation energies for the normal dimers. H. Lischka, *Chem. Phys. Lett.*, **20**, 448 (1973), has carried out high-accuracy calculations on He···H–OH and He···H–F. Lischka finds a greater interaction energy for He···F–H than He···H–F in contrast to Losonczy et al. who find a greater interaction energy for Ne···H–F than for Ne···F–H. Losonczy et al. interpret their calculations as a weak hydrogen bond while Lischka interprets his results as the $1/R^6$ and $1/R^7$ energy terms in a multipole expansion. The small interaction energies involved make further analysis of these interpretations inappropriate to this article.
(32) The cogent and systematic manner with which ionization potential lowerings in group 4, 5, 6, and 7 hydrides can be related to their electronic structure has been shown by A. W. Potts and W. C. Price, *Proc. R. Soc. London, Ser. A*, **326**, 181 (1972). In simple hydrides, the hydrogens do not distort the effective potential around the heavy atoms so that ΔI is solely a measure of the relative lone-pair energy and the ability of its orbital to interact with A–H (J. C. Slater, "Quantum Theory of Molecules and Solids", Vol. 1, McGraw-Hill, New York, N.Y., 1963, pp 133–134). The concept of lone-pair destabilization as an adjunct to hydrogen bonding is related to L. Hofacker's idea of lone-pair "loosening" (*Z. Naturforsch*, **13**, 1044 (1958)). This latter paper was the first quantitative attempt to treat the hydrogen bond within the molecular orbital framework.
(33) The highest occupied molecular orbitals of FH and ClH are doubly degenerate, but only that one in the A–H···B plane mixes into the hydrogen bonding molecular orbital of the dimers.
(34) P. Politzer, *J. Chem. Soc.*, **91**, 6235 (1969).
(35) In addition to the low ΔI for FH mentioned in the data available section, there is a basis set caused imbalance in the dipole moments of OH_2 and NH_3 relative to FH, thus the percent overestimate for NH_3 is more than double that for FH.
(36) Plots of $E_D \times R$ vs. diagonal averaged μ_{A-H} can be fitted by least squares to six lines all of whose slopes are close to $1.64\Delta I$. This match, along with Figure 9, provides internal numerical checks on eq 1.
(37) The units of K are $(\text{charge})^{-1}$. The quantity $K\Delta I$ may be thought of as energy lowering per unit charge. The appearance of ΔI instead of I in the E_D formula may be viewed as a means of making a first-order correction for differences in the energy integrals between second- and third-row atoms while still preserving the intuitive connection with I.
(38) As noted in the section on available data, R scales almost exactly to the known experimental values and the scale factor is absorbed in K.
(39) E_D values at optimized geometries for the nine dimers made from monomers NH_3, OH_2, FH also have been computed with the STO-3G basis (W. A. Lathan, L. A. Curtiss, W. J. Hehre, J. B. Lisle, and J. A. Pople, *Prog. Phys. Org. Chem.*, **11**, 175 (1974)). A least-squares fit to these results can be obtained which looks like the dashed lines of Figure 10 and a comparable fit by eq 1 can be realized using μ_{A-H} and ΔI computed from this basis. The STO-3G basis and resultant total energies, however, are notably inferior to the other data sets we have considered. There is insufficient flexibility in the basis for the lone-pair orbital tails to respond properly to the proton donors and for H_2N–H and HO–H this produces a reversal in order between electron donors NH_3 and OH_2. The relative magnitudes of the monomer dipole moments are also imperfect in STO-3G, e.g., $\mu(NH_3)$ is 25% greater than $\mu(FH)$ but experimental measurements give $\mu(NH_3)$ as 20% smaller than $\mu(FH)$. This basis defect shows up as H_2N–H and HO–H curves which are placed too low when experimental μ_{A-H} and ΔI are used in eq 1 to fit the computed results.
(40) It is interesting to note that eq 1 provides an equal or closer match to all sets of hydrogen bond E_D results than did analogous relationships to their available data for the six other physical models of structure used as examples in the introduction.
(41) Electrostatic potentials have proved quite useful in locating protonation sites. R. Bonaccorsi, C. Petrolongo, E. Scrocco, and J. Tomasi, "Quantum Aspects of Heterocyclic Compounds in Chemistry and Biochemistry", Vol. 2, E. D. Bergmann and B. Pullman, Ed., Academic Press, New York, N.Y., 1970, p 181; *Theor. Chim. Acta*, **20**, 321 (1970); R. Bonaccorsi, A. Pullman, E. Scrocco, and J. Tomasi, *Chem. Phys. Lett.*, **12**, 622 (1972). The success of predictions employing electrostatic potentials does not imply that the molecular interactions studied have a purely electrostatic origin.
(42) The large hump in the OH_2–FH regions follows from the large and almost equal values for the dipole moments of these monomers. The minimum at PH_3 and rise at ClH also follow directly from the relative dipole moment magnitudes. Higher angles for OH_2 and FH dimers and particularly for SH_2 and ClH reduce the maxima.
(43) The proton donor dipole points at B so $\cos\alpha = 1$.
(44) Charge transfer is probably the charge least influenced by the well-known shortcomings of Mulliken population analysis. Preliminary analysis of charge density difference plots shows contours of large increase and large decrease attached to B. Mulliken charges average these changes and overemphasize the changes on the hydrogen ligands of B. Thus δ_{BL} is indicative of the actual electron donor charge loss by both the hydrogens and the lone pair. None of the population analysis trend employed in this paper are contradicted by the difference plots.
(45) Just as in the case of dimerization energies, a given percent change in R produces an order of magnitude greater change in charge transfer than the same percent in θ. It is for this reason that the charge-transfer data can be organized to a high approximation by I alone without having to consider angular variation simultaneously.
(46) The dimers may be laid out linearly, thereby making comparisons easier, because the angular variation can be ignored to first order as mentioned in ref 45. A small effect that can also be ignored to first order is the slightly greater overlap of H by third-row lone pairs compared to second row. The effect of this on charge transfer is compensated by the larger third row r(A–H).
(47) The A atom is the dominant influence in A–H thus the fixed separation is R(A···B) rather than r(H···B).
(48) For all dimers the electron donors are placed at the coordinate origin with their symmetry axis directed horizontally. The vertical axis is the hydrogen-bonding lone-pair direction for OH_2, SH_2, FH, and ClH and the horizontal axis is the lone-pair direction for NH_3 and PH_3. The hydrogen bond angle, θ, is measured counterclockwise from the horizontal axis.
(49) It should also be noted that the electronegativity of B, χ_B, is not a useful parameter for organizing trends in dimerization energies between rows nor in charge rearrangements. $\chi_F > \chi_N$ but $\delta_N > \chi_F$; $\chi_{Cl} > \chi_N$ but $\delta_N \gg \delta_{Cl}$.
(50) Ligand charge buildup is proportional to the number of A ligands, but even for H_2N–H and H_2P–H charge accumulation on the ligands is of the same sign and decidedly smaller magnitude than on A itself. Another way to arrive at the same conclusion comes from examining dimer dipole moment components perpendicular to A–H···B for $BH_n = NH_3$ and PH_3. In all 12 such dimers $\theta = 0°$ and the proton donor dipole moment component perpendicular to A–H is obtainable. For a specified A–H the perpendicular component is almost identical for NH_3 and PH_3 and it is almost identical with the monomer values. This implies little change on A ligands on dimer formation.
(51) Penetration of the proton donor valence orbital tails into the H···B region parallels H orbital occupancy, i.e., the A valence orbital amplitudes at H, both in absolute value and as a percent of radial maximum, decrease in the order N, O, F, and P, S, Cl. A smaller amplitude at H allows greater lone-pair overlap before Pauli exclusion comes into play.
(52) The off-graph data point shown is the distortion of the second row μ_D that results at H_2N–H from the inferior F wave function in $HFHNH_2$. Extrapolation was based on using the other eight dimers. Present quantum mechanical calculations are also too crude to give quantitative details for trends in either the ratio or difference between the dimer dipole and the vector sum of monomer moments.
(53) Each of the three individual curves has a similar shape and dependence on A–H because R is almost constant within a row.
(54) R. S. Mulliken, *J. Chem. Phys.*, **2**, 782 (1934); **3**, 573 (1935).
(55) J. E. Del Bene, *J. Chem. Phys.*, **56**, 4923 (1972); **57**, 1899 (1972); **58**, 926, 3139 (1973); *J. Am. Chem. Soc.*, **95**, 5460 (1973).
(56) M. J. T. Bowers and R. M. Pitzer, *J. Chem. Phys.*, **59**, 163 (1973).
(57) F. B. van Duijneveldt and J. N. Murrell, *J. Chem. Phys.*, **46**, 1759 (1967); F. B. van Duijneveldt, *Ibid.*, **49**, 1424 (1968); J. G. C. M. van Duijneveldt-van de Rijdt and F. B. van Duijneveldt, *Chem. Phys. Lett.*, **2**, 565 (1968); *Theor. Chim. Acta*, **19**, 83 (1970); *J. Chem. Soc.*, **93**, 5644 (1971). The perturbation method is given in J. N. Murrell and G. Shaw, *J. Chem. Phys.*, **46**, 1768 (1967).
(58) M. Dreyfus and A. Pullman, *Theor. Chim. Acta*, **19**, 20 (1970). The many interesting ideas and graphs in this paper are especially notable.
(59) K. Morokuma, *J. Chem. Phys.*, **55**, 1236 (1971); S. Yanube and K. Morokuma, *J. Am. Chem. Soc.*, **97**, 4458 (1975).
(60) P. A. Kollman and L. C. Allen, *Theor. Chim. Acta*, **18**, 399 (1970).
(61) A. T. Hagler, E. Huber, and S. Lifson, *J. Am. Chem. Soc.*, **96**, 5319 (1974); A. T. Hagler and S. Lifson, *Ibid.*, **96**, 5327 (1974).
(62) The appropriate intermuclear separation variable here is r(H···B) rather than R(A···B) because r(H···B) eliminates the problem of the different range of r(A–H) values between the second and third rows. This provides a closer match between the second and third rows for a given electron donor and leads to simpler and more easily analyzed patterns (e.g., Figures 2, 3, 17, 21, and 22). On the other hand, it is A more than H which determines the physical response of the proton donor and thus R(A···B) rather than r appears in the dimerization energy formula and in other situations such as the nonequilibrium geometry calculations.
(63) A basis set imbalance in PH_3 relative to the other monomers leads to a slight excess charge on the hydrogens. This leads to r values which are too large and especially affects electron donors NH_3 and OH_2 because of their large ΔI. Thus r for H_2PHNH_3 and H_2PHOH_2 (shown by the two small circles in Figure 17) are out of line and extrapolation based on the other data leads to r(H···N) = 2.62 Å and r(H···O) = 2.57

Å. Use of the original computed data does not change any conclusions.

(64) r(H···B) and R(A···B) are entirely equivalent for this consideration.

(65) Most of the relevant part of the lone pair is quite far from the B nucleus implying that a Coulombic potential may be a reasonable assumption.

(66) The nature of the effective potential in atoms has been approached through the study of Z_p and Z_I and these lead one to expect a dependence within the range investigated here. An extended discussion of this problem is given in J. C. Slater, "Quantum Theory of Atomic Structure", Vol. 1, McGraw-Hill, New York, N.Y., 1960, Chapter 9.

(67) The argument presented here is an approximation to the total energy curve and it compares R values rather than determining absolute magnitudes. Thus it does not bear on the energy difference quantity E_D.

(68) The most accurate dimer calculations (H. Popkie, H. Kistenmacher, and E. Clementi, *J. Chem. Phys.*, **59**, 1325 (1973); G. H. F. Diercksen, *Theor. Chim. Acta*, **21**, 335 (1971); G. H. F. Diercksen and W. P. Kraemer, *Chem. Phys. Lett.*, **5**, 419 (1970)) do not yield tetrahedral angles. The two gas phase dimers for which experimental geometries are known (T. R. Dyke and J. S. Muenter, private communication on $(H_2O)_2$; T. R. Dyke, B. J. Howard, and W. Klemperer, *J. Chem. Phys.*, **56**, 2442 (1969)) show angles reasonably close to tetrahedral. However, compilations of experimental data (e.g., J. Donohue, "Structural Chemistry and Molecular Biology", A. Rich and N. Davidson, Ed., W. H. Freeman, San Francisco, Calif., 1969, p 443) and all of the sets of calculations show wide variation in angle for a specified electron donor and this is not expected if lone-pair hybrid orbitals were solely responsible for directionality.

(69) P. A. Kollman, *J. Am. Chem. Soc.*, **94**, 1837 (1972), has discussed directionality as a compromise between charge transfer from the lone pair and electrostatics. He also discussed relative lone-pair charge transfer on the basis of occupied $\sigma-\pi$ orbital energy differences.

(70) We describe the interaction in terms of dipole moments, but charge density difference plots show some evidence of quadrupole–quadrupole interactions as well. The monomers all have quadrupole moments large enough to give almost comparable interaction magnitudes in some cases.

(71) The higher angles observed for third-row over the second-row H_nB are intrinsic properties of the monomers. For example, at a radius of 90% enclosed charge, the electron distribution in the $p\pi$ orbital of HF is similar to that in HCl, but HF has almost twice the dipole moment with $\frac{3}{4}$ the internuclear separation of HCl. This means that the potential energy seen by a point positive charge at hydrogen bond distances will be lowest at low angles for HF and at higher angles for HCl (even though their quadrupole moments are almost the same). This is the situation that Kollman et al.[17] find from their electrostatic potential calculations. The large HF dipole compared to HCl is a manifestation of the difference in $\pi-\sigma$ separation noted by these authors.

(72) R. M. Badger, *J. Chem. Phys.*, **2**, 128 (1934); **3**, 710 (1935). If one specifies an E_D and R in a Morse curve representation of a particular hydrogen bond and then asks for a stretching force constant comparison with a covalent bond, it is not possible to get a unique answer because criteria for matching the curve shapes are not unique.

(73) L. A. Curtiss and J. A. Pople, *J. Chem. Phys.*, in press.

(74) G. C. Pimentel and A. L. McClellan, "The Hydrogen Bond", W. H. Freeman, San Francisco, Calif., 1960, p 135.

(75) The finding that Badger's rule encompasses hydrogen bonds is supported by the Hagler and Lifson result[61] that a Lennard-Jones potential plus Coulomb terms with the same parameters as those employed in ordinary, nonhydrogen bonding interatomic interaction potentials is able to represent the amide hydrogen bond.

(76) The group 6 value in (4) is larger than the second-row Badger's rule value of 0.68 used in our $(H_2O)_2$ example. For $d_{OO} = 0.80$, $K_{OO} = 0.17$ and this difference is negligible compared to the much greater uncertainties in available data.

(77) J. E. Del Bene and J. A. Pople, *J. Chem. Phys.*, **52**, 4848 (1970); P. A. Kollman and L. C. Allen, *ibid.*, **51**, 3286 (1969).

(78) J. E. Del Bene and J. A. Pople, *J. Chem. Phys.*, **55**, 2296 (1971); P. A. Kollman and L. C. Allen, *ibid.*, **52**, 5085 (1970).

(79) E. R. Lippincott and R. Schroeder, *J. Chem. Phys.*, **23**, 1099, 1131 (1955).

(80) All of the high-accuracy calculations for E_D and K_{AB} have been carried out on $(HF)_2$ and $(H_2O)_2$. Unfortunately, the E_D values for these two dimers are too close to serve as a useful guide to the validity of this hypothesis.

(81) The trends of $(K_{AH})_D/(K_{AH})_M$ for fixed BH_n within a given row can also be understood in terms of the internuclear separation, R(A···B). The data for nonequilibrium geometries in Table VII showed that charge on A is dependent almost solely on the distance between A and the lone pair. Thus δ_A is inversely proportional to R and R is smaller for F–H than H_2N–H. We have demonstrated previously, however, that the equilibrium internuclear separation is determined by μ_{A-H}, therefore these viewpoints are interlocked.

(82) G. Govil, A. D. H. Clague, and H. J. Bernstein, *J. Chem. Phys.*, **49**, 2821 (1968); *Can. J. Chem.*, **47**, 625 (1969). These authors have related chemical shifts and other readily measurable quantities to dimerization energy and they have obtained estimates for the methanol dimer, methanol–trimethylamine, and hydrogen chloride–dimethyl ether.

(83) The simple idea of connecting downfield shift to the loss of charge on the hydrogen may have some utility, but the magnitude of the loss appears too small to account for the observed shifts,[2] and, in addition, the long-standing quantum mechanical question of how to partition molecular charge distributions may be especially difficult in this case.

(84) It has been pointed out (P. A. Kollman, private conversation) that in a localized orbital representation lone-pair dipole moments make the major contribution to the monomer dipole moment and therefore will dominate in determining the bond dipole moment.

(85) σ molecular orbitals are necessary for explaining at least part of directionality (e.g., second- vs third-row electron donors for fixed A–H) and this was expressed in our model by use of the BH_n dipole moment.

(86) A. W. Potts and W. C. Price, *Proc. R. Soc. London, Ser. A*, **326**, 181 (1972).

(87) D. W. Turner, C. Baker, A. D. Baker, and C. R. Brundle, "Molecular Photoelectron Spectroscopy", Wiley-Interscience, New York, N.Y. 1970.

(88) J. E. Del Bene, *Chem. Phys. Lett.*, **24**, 203 (1974).

(89) W. J. Hehre, R. F. Stewart, and J. A. Pople, *J. Chem. Phys.*, **51**, 2657 (1969).

(90) J. E. Del Bene, *J. Chem. Phys.*, **57**, 1899 (1972).

(91) J. E. Del Bene and J. A. Pople, *J. Chem. Phys.*, **55**, 2296 (1971).

(92) J. E. Del Bene and J. A. Pople, *J. Chem. Phys.*, **52**, 4858 (1970).

(93) H. Kistenmacher, H. Popkie, and E. Clementi, *J. Chem. Phys.*, **58**, 5627 (1973).

(94) R. J. Zollweg, *J. Chem. Phys.*, **50**, 4251 (1969).

(95) W. P. Kraemer and G. H. Diercksen, *Chem. Phys., Lett.*, **5**, 570 (1970).

(96) Although a consistent set of calculations with a good basis is not presently available, extrapolation suggests the following sequence of approximate internuclear separations: HF···H–F, $R = 2.75$ Å; F^-···H–F, $R = 2.50$ Å; $(F{\cdots}H{\cdots}F)^-$, $R = 2.25$ Å, thus indicating a 0.5 Å shortening between normal and strongest hydrogen bonds.

(97) P. N. Noble and R. N. Kortzeborn, *J. Chem. Phys.*, **52**, 5375 (1970).

(98) S. A. Harrell and D. H. McDaniel, *J. Am. Chem. Soc.*, **86**, 4497 (1964).

(99) A. Stφgard, A. Strich, J. Almlöf, and B. Roos, *Chem. Phys.*, in press. This calculation employed a medium sized s,p basis and also included a configuration interaction treatment. At the SCF level a slightly lower energy was obtained for an incorrect asymmetric geometry and it is not known whether this comes about from a basis set limitation or is intrinsic to the Hartree-Fock approximation. The electron affinity of OH is not known accurately and we have arbitrarily assigned a value of 1.0 eV. Our result would only change by 1.0 kcal/mol for a 1.0 eV change in ΔI.

(100) P. N. Noble and G. C. Pimentel, *J. Chem. Phys.*, **49**, 3165 (1968); V. Bondybey, G. C. Pimentel, and P. N. Noble, *ibid.*, **55**, 540 (1971); P. N. Noble, *ibid.*, **56**, 2088 (1972).

(101) S. V. O'Neil, H. F. Schaeger III, and C. F. Bender, *Proc. Natl. Acad. Sci. U.S.*, **71**, 104 (1974). This article also contains references to the controversy that exists with respect to the experimental measurements.

(102) E. Clementi, *J. Chem. Phys.*, **46**, 3851 (1967); **46**, 2323 (1967); E. Clementi and J. N. Gayles, *ibid.*, **47**, 3837 (1967).

(103) The empirical bond energy–bond order method has been applied to ClHCl yielding a stable species bound by 1.56 kcal/mol (D. G. Truhlar, P. C. Olson, and C. A. Parr, *J. Chem. Phys.*, **57**, 4479 (1972)). This scheme also predicts an unstable symmetrical FHF radical with a barrier height of 5.6 kcal/mol.

(104) J. E. Del Bene, *J. Am. Chem. Soc.*, **95**, 5460 (1973), NH_3; *J. Chem. Phys.*, **57**, 1899 (1972), OH_2; *ibid.*, **58**, 3139 (1973) OCH_2.

(105) The value of q_H for NH_2O–H given by Del Bene (ref 104) is too large compared with the other q_H and it is not known whether this is the result of the STO-3G basis or is a basic structural feature of the monomer. q_0 for NH_2O–H is too small in the same proportion as q_H is too large, yielding $(E_D)(R)$ values in line with the other proton donors and thereby acting as if q_H for NH_2O–H fitted the straight lines determined by the other q_H.